Supplementary Information

Structure-Function Relationships in Pure Archaeal Bipolar Tetraether Lipids

Ahanjit Bhattacharya,[a, b] Isaac D. Falk,[a] Frank R. Moss III,[c] Thomas M. Weiss,[d] Khoi N. Tran,[a] Noah Z. Burns,[a,] * Steven G. Boxer[a,*]

[a]Department of Chemistry, Stanford University, Stanford, CA 94305

[b]Stanford Center for Innovation in Global Health, Stanford University, Stanford, CA-94305

[c]Linac Coherent Light Source, SLAC National Accelerator Laboratory, Menlo Park, CA 94025

[d]Stanford Synchrotron Radiation Laboratory, SLAC National Accelerator Laboratory, Menlo Park, CA 94025

* Correspondence to: sboxer@stanford.edu, nburns@stanford.edu

Materials and Methods

Chemicals and general considerations

All organic synthesis reactions were conducted in oven-or flame-dried glassware under an atmosphere of nitrogen or argon unless otherwise noted. Commercial reagents and solvents were used as received unless otherwise noted with the exception of the following: DMF, toluene, tetrahydrofuran, methanol, benzene, and dichloromethane were dried by passing through a bed of activated alumina in a JC Meyer Solvent System. Glucosyl donor **Glc1** was prepared as described previously.[1] Flash column chromatography was performed using F60 silica gel (40-63 μm, 230-400 mesh, 60 Å) purchased from Silicycle. DPhPA, DPhPC, DoPhPC, DPhPG, dipalmitoyl phosphatidylcholine (DPPC), palmitoyl oleoyl phosphatidylcholine (POPC), dioleoyl phosphatidylethanolamine (DOPE), cholesterol, and 16:0 Biotinyl Cap PE were purchased from Avanti Polar Lipids (Alabaster, AL). DPhPC was purchased from Cayman Chemicals. Texas Red-1,2-dihexadecanoyl-*sn*-glycero-3-phosphoethanolamine (TR-DHPE), Atto 647N-DMPE, and NeutrAvidin were purchased from Thermo Fisher Scientific. Sulforhodamine B (SRB), pyranine (HPTS), disialoganglioside GD1a (from bovine brain), octyl glucoside, and Sepharose CL-4B were purchased from Sigma-Aldrich. Tris.HCl, HEPES buffer, buffer salts, sucrose, and glucose were obtained from Fisher Scientific and Sigma-Aldrich. Polydimethylsiloxane was obtained from Ellsworth Adhesives (Hayward, CA). Poly(L-lysine)-graft-poly(ethylene glycol) and Poly(L-lysine)-graft-poly(ethylene glycol) biotin were purchased from SuSoS (Dübendorf, Switzerland). Structures of various non-GDGT lipids described in this study are shown below:

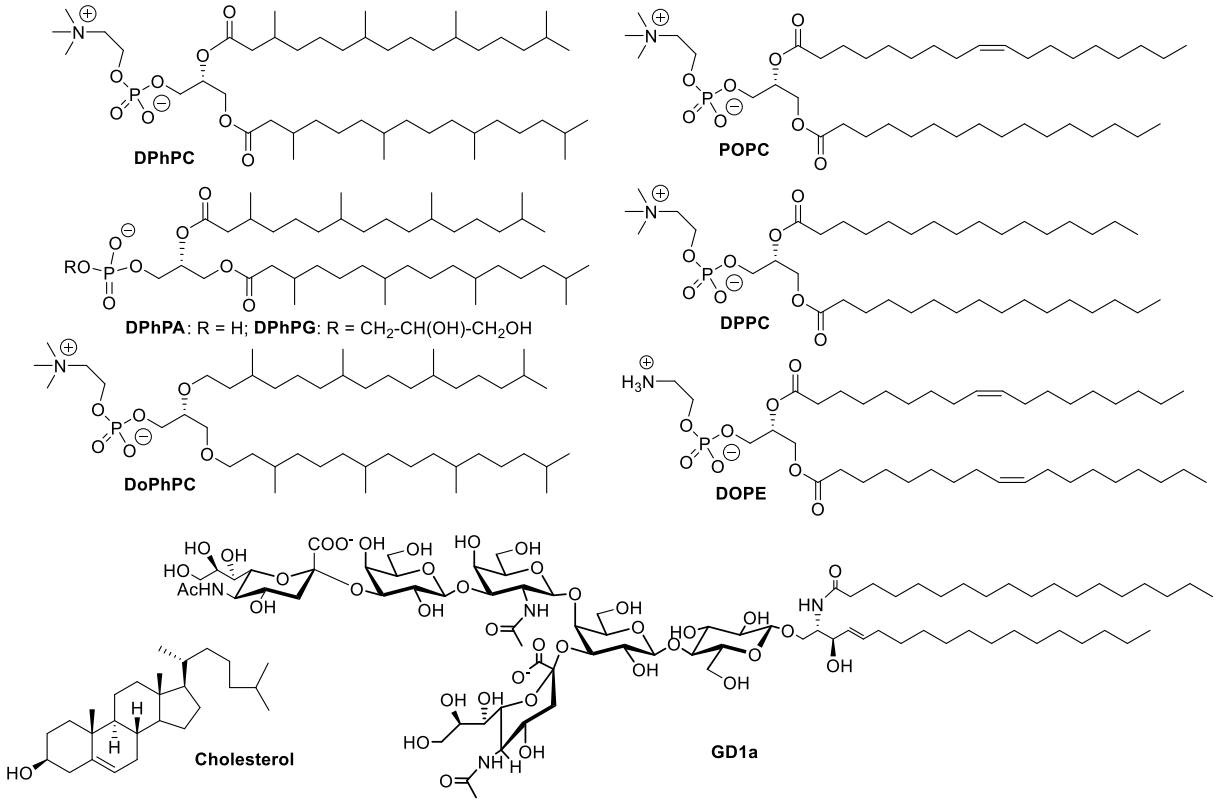

The following abbreviations have been used in synthetic methodologies for common words and phrases: RT – room temperature, sat. – saturated, equiv – equivalent, minute(s) – min, hour(s) – h.

Compound characterization

Proton nuclear magnetic resonance (^{1}H NMR), carbon nuclear magnetic resonance (^{13}C NMR), and phosphorus nuclear magnetic resonance spectra were recorded on Varian Inova 600, Varian Inova 500, or Varian Mercury 400 spectrometers operating respectively at 600, 500, and 400 MHz for ^{1}H and at 150, 125, and 100 MHz for ^{13}C and at 162 MHz for ^{31}P. Chemical shifts are reported in parts per million (ppm) with respect to residual protonated solvent for ^{1}H ($CHCl_3$ = δ 7.26, MeOH = δ 3.31) and with respect to carbon resonances of the solvent for ^{13}C ($CDCl_3$ = δ 77.0, CD_3OD = δ 49.0). Peak multiplicities are annotated as follows: app = apparent, br = broad, s = singlet, d = doublet, t = triplet, q = quartet, p = quintet, m = multiplet. Infrared (IR) spectra were recorded on a Nicolet 6700 FT-IR spectrometer. Optical rotations were measured using a JASCO P-2000 polarimeter. Standard HRMS data were collected on a Waters Micromass 70-VSE mass spectrometer, an Agilent QTOF tandem liquid chromatography-mass spectroscopy (LC-MS) instrument or a Micromass 70-VSE EI/CI/FD/FI mass spectrometer. Analytical thin-layer chromatography (TLC) was carried out on 250 μm 60-F_{254} silica gel plates purchased from EMD Millipore, and visualization was affected by observation of fluorescence-quenching with ultraviolet light and staining with *p*-anisaldehyde, phosphomolybdic acid with cerium sulfate (Seebach's stain), potassium permanganate ($KMnO_4$ stain), or cerium ammonium molybdate (CAM stain) as a developing agent.

Synthetic Procedures

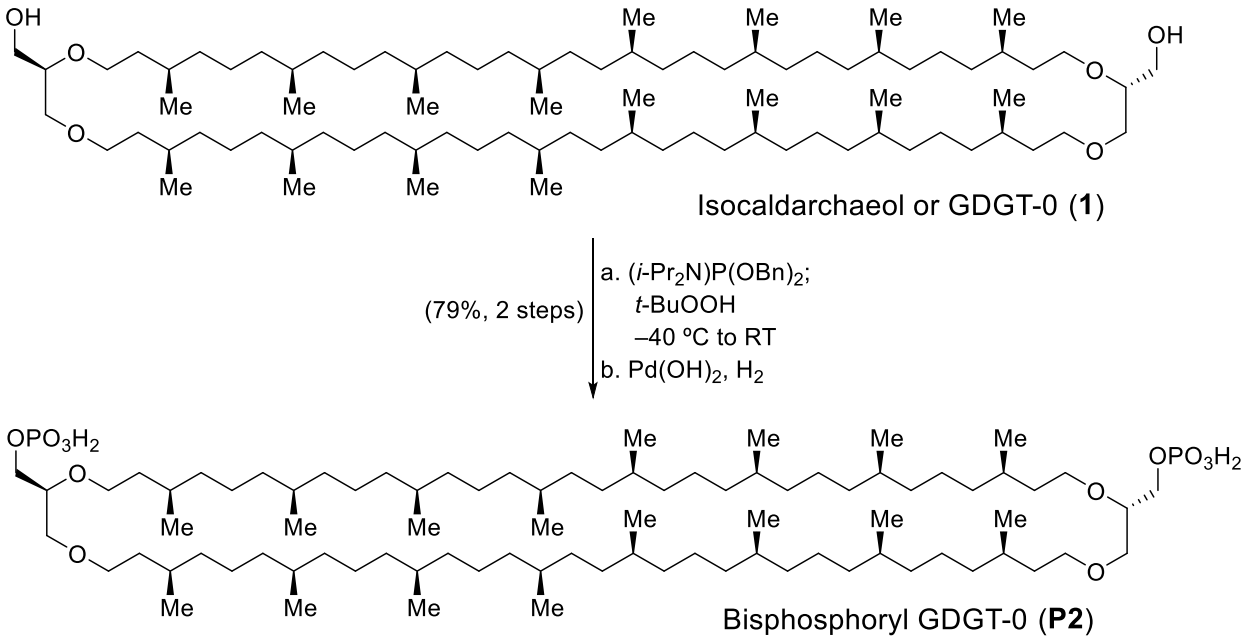

Scheme S1. Reaction scheme for synthesizing bisphosphoryl GDGT-0 (**P2**).

Bisphosphoryl GDGT-0 (**P2**) (Scheme S1): To a solution of GDGT-0 (**1**) (11.3 mg, 8.68 µmol, 1.0 equiv) in anhydrous and degassed CH_2Cl_2 (0.1 mL) in a screw cap vial was added a 0.45 M solution of tetrazole in acetonitrile (154 µL, 69.4 µmol, 8.0 equiv). To this solution was added dibenzyl *N,N*-diisopropylphosphoramidite (15.0 mg, 43.4 µmol, 5.0 equiv) as a solution in anhydrous and degassed CH_2Cl_2 (0.1 mL). The septum was replaced with a screw cap and the reaction was stirred at RT for approximately 14 h. The screw cap was replaced with a septum equipped with a balloon of argon and the reaction was cooled to -40 °C. A 5.5 M solution of *t*-butyl hydroperoxide in decane (31.6 µL, 174 µmol, 20.0 equiv) was added to the solution. The reaction was slowly warmed to RT over 4 h at which point TLC indicated full conversion. The reaction mixture was concentrated *in vacuo* and the crude residue was purified by preparative TLC on silica gel (35% EtOAc/hexanes, run twice) to afford the benzylated GDGT-0 bisphosphate (*structure not shown*) intermediate which was used directly in the next step.

The benzylated GDGT-0 bisphosphate was suspended in degassed and anhydrous solution of 1:1 THF/EtOH (1 mL). A small amount of 20% $Pd(OH)_2/C$ (~1 mg, 1.4 µmol, 0.16 equiv) was added to the solution and the reaction was sparged with H_2 for approximately 5 min after which the reaction was stirred under an atmosphere of H_2 for approximately 15 h. The reaction mixture was passed over a plug of celite with Et_2O and concentrated. The crude residue was purified using a column of Sephadex LH-20 (33-66% $CHCl_3$/MeOH) to afford the desired bisphosphoryl GDGT-0 (**P2**) (10.0 mg, 79% yield over two steps).

Spectroscopic data matched that reported in the literature.[2]

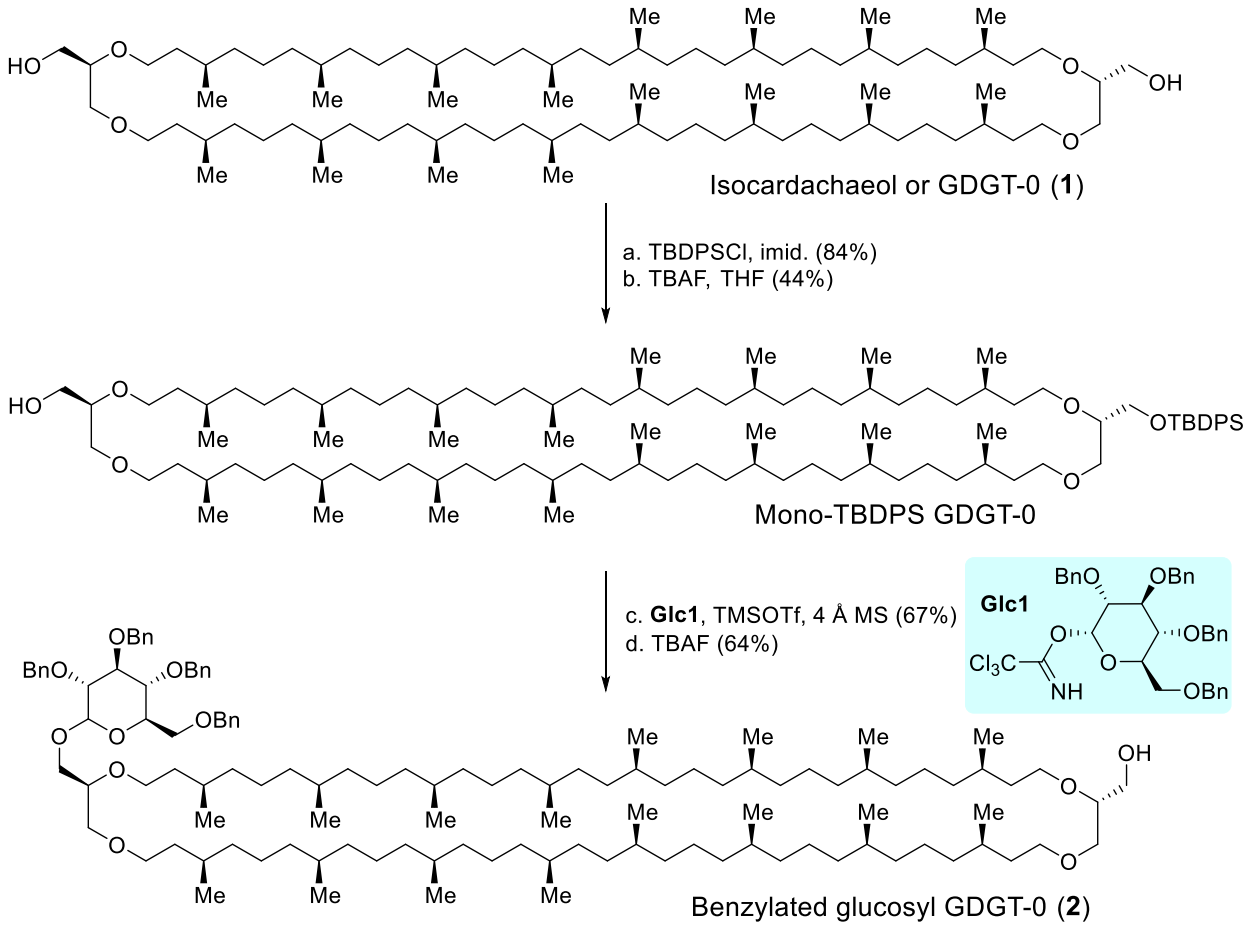

Scheme S2. Reaction scheme for synthesizing benzylated glucosyl GDGT-0 (**2**).

Benzylated glucosyl GDGT-0 (2) [Mixture of anomers]: (Scheme S2) To a solution of **1** (33.4 mg, 25.6 µmol, 1.0 equiv) in CH_2Cl_2 (0.2 mL) was added imidazole (6.9 mg, 103 µmol, 4.0 equiv) and *t*-butyl(chloro)diphenylsilane (20 µL, 76.9 µmol, 3.0 equiv). After stirring 15 h at RT, TLC indicated full conversion. The reaction mixture was diluted with CH_2Cl_2 (1 mL) and washed with 1 N HCl (1×1 mL), sat. aq. $NaHCO_3$ (1×1mL) and sat. aq. NaCl (1×1 mL). Each aqueous layer was extracted once with the same portion of CH_2Cl_2 (1×1 mL). The combined organic layers were dried over Na_2SO_4 and concentrated *in vacuo*. The crude residue was purified via flash column chromatography on silica gel (2-10% EtOAc/hexanes) to afford the desired bis-TBDPS GDGT-0 intermediate (38.4 mg, 84%) (*structure not shown*) which was used directly in the next step. The bis-TBDPS GDGT-0 (38.4 mg, 21.6 µmol, 1.0 equiv) was suspended in THF (1 mL) and a 0.1 M solution of TBAF in THF (216 µL, 21.6 µmol, 1.0 equiv) was added dropwise to the solution. The reaction was closely monitored by TLC (every 10 min) until the major species present was the desired mono-TBDPS GDGT-0 (approximately after 40 min of reaction). The reaction was quenched with a 1:1 mixture of sat. aq. $NaHCO_3$/sat. aq. NaCl (1×1 mL) and was extracted with EtOAc (3×1 mL). The combined organic layers were dried over Na_2SO_4 and concentrated *in vacuo*. The crude residue was purified using flash chromatography on silica gel (2-30% EtOAc/hexanes) to afford the desired mono-TBDPS GDGT-0 (14.7 mg, 44% yield) which was used directly in the next step. Bis-TBDPS GDGT-0 (~14 mg) and **1** (~7 mg) were also recovered from the reaction.

Mono-TBDPS GDGT-0 (14.7 mg, 8.59 μmol, 1.0 equiv) and **Glc1** (12.4 mg, 18.0 μmol, 2.1 equiv) were concentrated from toluene into a vial. 4 Å molecular sieves were added to the vial and the mixture was suspended in anhydrous CH_2Cl_2 (0.2 mL). To this solution was added a 1% v/v solution of TMSOTf in CH_2Cl_2 (15.9 μL, 0.859 μmol, 0.1 equiv). The reaction was stirred for 1.25 h at RT until TLC indicated full conversion. A few drops of Et_3N were then added to the reaction. The reaction mixture was directly purified via preparative TLC on silica (15% EtOAc/hexanes) to afford the TBDPS/benzylated glucosyl GDGT-0 (12.0 mg, 68%) (*structure not shown*) which was used directly in the next step.

The TBDPS/benzylated glucosyl GDGT-0 (12.0 mg, 5.82 μmol, 1.0 equiv) was dissolved in THF (1 mL) and a 1.0 M solution of TBAF in THF (29 μL, 29.1 μmol, 5.0 equiv) was added. After stirring at RT for 3 h, TLC indicated full conversion. The reaction mixture was diluted with EtOAc (1 mL) and washed with a 1:1 solution of sat. aq. $NaHCO_3$/sat. aq. NaCl (1×1 mL). The aqueous layer was further extracted with EtOAc (2×1 mL). The combined organic layers were dried over Na_2SO_4 and concentrated *in vacuo*. The resulting crude residue was purified using preparative TLC on silica gel (20% EtOAc/hexanes) to afford the benzylated glucosyl GDGT-0 (**2**) (6.8 mg, 64%, 1.6:1 ratio of α/β anomers as determined in the next step).

Physical Properties: Colorless oil

R_f = 0.23 (silica gel, 15% EtOAc/Hexanes, visualized CAM stain)

IR (film) 3444 (br), 2922, 2851,1712, 1456, 1376, 1260, 1093 (br), 1070, 803, 732, 696 cm^{-1}

^{1}H NMR (600 MHz, $CDCl_3$) δ 7.39-7.24 (m, 18H), 7.14 (t, *J* = 8.4 Hz, 2H), 5.02-4.40 (m, 9H), 3.97 (m, 1H), 3.87-3.39 (m, 23H), 2.14 (t, *J* = 6.3 Hz, 1H), 1.60 (m, 4H), 1.53 (m, 4H), 1.41-0.98 (m, 97H), 0.91-0.81 (m, 48H);

^{13}C NMR (126 MHz, $CDCl_3$) δ 138.90, 138.65, 138.56, 138.49, 138.42, 138.20, 138.16, 137.99, 128.36, 128.32, 128.26, 128.11, 127.94, 127.88, 127.87, 127.75, 127.70, 127.62, 127.56, 127.51, 103.91, 97.31, 84.69, 82.17, 82.01, 80.05, 78.35, 78.01, 77.84, 77.79, 77.65, 75.66, 75.61, 74.97, 74.89, 74.64, 73.50, 73.45, 72.80, 71.09, 70.92, 70.16, 70.08, 69.99, 69.92, 68.89, 68.83, 68.58, 68.48, 67.85, 63.08, 37.52, 37.40, 37.37, 37.13, 37.06, 36.71, 36.66, 36.58, 34.31, 33.06, 32.79, 29.92, 29.83, 29.79, 29.76, 29.69, 24.47, 24.40, 24.37, 19.83, 19.80 [Multiple signals are missing. There are multiple signals with greater intensity suggesting the contribution of multiple nuclei]

HRMS (ES+): calculated for $C_{120}H_{206}O_{11}Na$ $[M+Na]^+$ 1846.55, found 1846.55

$[\alpha]_D^{23}$ = +8.68 (c = 0.24, $CHCl_3$)

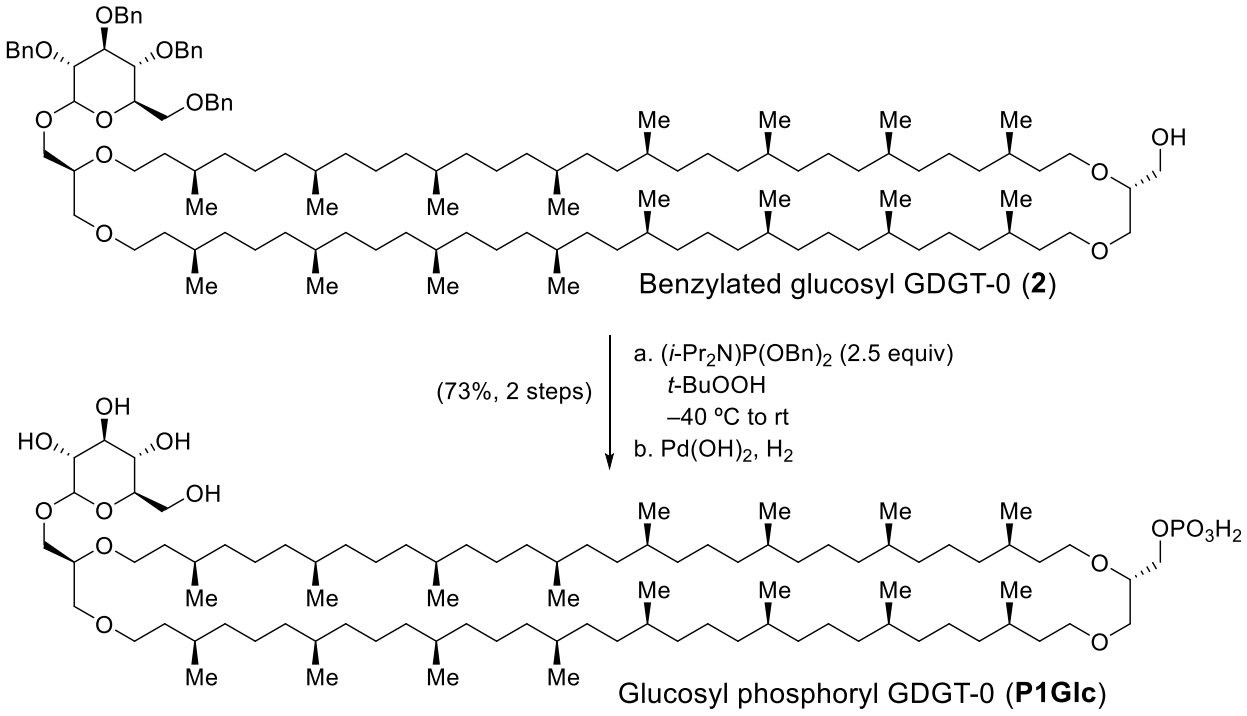

Scheme S3. Reaction scheme for synthesizing glucosyl phosphoryl GDGT-0 (**P1Glc**).

Glucosyl phosphoryl GDGT-0 (**P1Glc**) [Mixture of anomers] (Scheme S3): To a solution of benzylated glucosyl GDGT-0 (**2**) (6.8 mg, 3.7 µmol, 1.0 equiv) in anhydrous and degassed CH_2Cl_2 (0.1 mL) in a screw cap vial was added a 0.45 M solution of tetrazole in acetonitrile (33 µL, 15 µmol, 4.0 equiv). To this solution was added dibenzyl *N,N*-diisopropylphosphoramidite (3.2 mg, 9.3 µmol, 2.5 equiv) as a solution in anhydrous and degassed CH_2Cl_2 (0.1 mL) and the septum was replaced by a screw cap. The reaction was stirred at RT for ~15 h. TLC indicated full conversion and a balloon of argon gas was affixed to the vial. The reaction was subsequently cooled to -40 °C. To this solution was added a 5.5 M solution of *t*-butyl hydroperoxide in decane (10 µL, 54.4 µmol, 14.7 equiv). The reaction mixture was allowed to slowly warm to RT over 5 h. TLC indicated full conversion to the desired product and the reaction mixture was directly loaded onto a silica gel preparative TLC plate. The reaction was then purified using preparative TLC on silica gel (20% EtOAc/hexanes) to afford the benzyl-protected phosphate ester which was used directly in the next step.

The benzyl-protected phosphate ester was suspended in a 1:1 mixture of degassed THF/EtOH (1 mL). To the solution was added a small amount of 20% $Pd(OH)_2/C$ (~1 mg, 1.4 µmol, 0.38 equiv). H_2 was bubbled through the solution for 5 min and then the reaction was stirred under an atmosphere of H_2 for ~18 h. The reaction mixture was then passed over celite with MeOH and concentrated *in vacuo*. The crude residue was passed over a column of Sephadex LH-20 using 10% MeOH/$CHCl_3$ as the eluent to afford the desired product glucosyl GDGT-0 phosphate (**P1Glc**) (4.2 mg, 73% yield over 2 steps, 1.6:1 ratio of α/β anomers).

Physical Properties: Colourless oil (hygroscopic, forms white wax upon standing in air)

IR (film) 3393 (br), 2953, 2922, 2852, 1715, 1655, 1461, 1377, 1260, 1053 (br), 908, 801, 734

^{1}H NMR (600 MHz, 8:1 $CDCl_3/CD_3OD$) δ 4.74 (d, *J* = 3.6 Hz, 0.55H, α-anomer), 4.21 (d, *J* = 7.7 Hz, 0.33H β-anomer), 3.86 (m, 2H), 3.70 (m, 2H), 3.55 (m, 11H), 3.37 (m, 4H), 3.29 (m, 4H), 3.21 (m, 1H) [This region is partially obscured by the residual solvent signal of CD_3OD, attempts to

dissolve the sample in other common deuterated solvents were unsuccessful], 1.52 (m, 4H), 1.44 (m, 4H), 1.35-0.91 (m, 101H), 0.83-0.78 (m, 12H), 0.78-0.74 (m, 36H)

^{13}C NMR (126 MHz, 8:1 $CDCl_3/CD_3OD$) δ 103.25 (β-anomer), 98.76 (α-anomer), 77.67, 76.02, 75.77, 73.92, 73.37, 72.15, 71.65, 70.41, 70.20, 69.93, 69.81, 68.96, 68.75, 68.51, 67.01, 64.91, 61.66, 61.40, 37.31, 37.21, 36.73, 36.67, 36.46, 36.40, 34.11, 32.88, 32.61, 29.72, 29.59, 29.51, 24.29, 24.27, 24.23, 19.63, 19.58, 19.50, 19.47 (Due to limited amounts of material, signals were confirmed through HSQC) [Multiple signals are missing. There are multiple signals with greater intensity suggesting the contribution of multiple nuclei]

^{31}P NMR (162 MHz, 8:1 $CDCl_3/D_3COD$) δ 0.74

HRMS (ES+) calculated for $C_{92}H_{183}O_{14}NaP$ $[M+Na]^+$ 1566.33, found 1566.32

$[\alpha]_D^{23}$ = +4.1 (c = 0.1, 8:1 $CHCl_3$/MeOH)

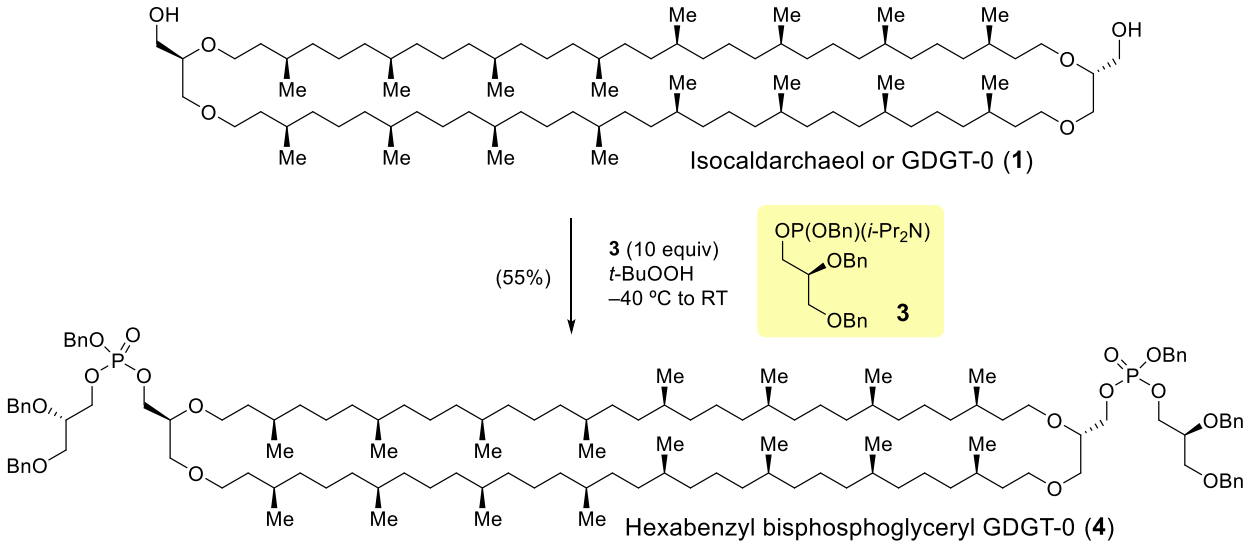

Scheme S4. Reaction scheme for synthesizing hexabenzyl bisphosphoglyceryl GDGT-0 (**4**).

Hexabenzyl bisphosphoglyceryl GDGT-0 (4) (Scheme 4): To a solution of GDGT-0 (**1**) (20.0 mg, 15.4 μmol, 1.0 equiv) in anhydrous CH_2Cl_2 (0.3 mL) in a screw cap vial was added phosphoramidite **3** (78.3 mg, 154 μmol, 10.0 equiv). To this solution was added 0.45 M solution of tetrazole in acetonitrile (600 μL, 270 μmol, 17.6 equiv) and the septum was replaced by a screw cap. The reaction was stirred at RT for ~15 h. TLC indicated full conversion and the reaction was cooled to -40 °C. To this solution was added a 5.5 M solution of *t*-butyl hydroperoxide in decane (84 μL, 460 μmol, 30 equiv). The reaction was allowed to stir at -40 °C and was then rapidly warmed to RT and allowed to react for another 3 h. The reaction mixture was concentrated *in vacuo* and directly loaded onto a silica gel preparative TLC plate. The reaction was then purified using preparative thin layer chromatography on silica gel (40% EtOAc/hexanes) to afford **4** (18.8 mg, 57% yield).

Physical Properties: Colourless oil

R_f = 0.45 (silica gel, 40% EtOAc/hexanes, visualized with CAM stain)

^{1}H NMR (600 MHz, $CDCl_3$) δ 7.40-7.20 (m, 30H), 5.05 (dd, *J* = 7.9, 4.7 Hz, 4H), 4.77-4.58 (m, 4H), 4.51 (d, *J* = 3.1 Hz, 4H), 4.22 (m, 2H), 4.18-3.95 (m, 6H), 3.86-3.75 (m, 2H), 3.65-3.49 (m, 10H), 3.43 (m, 8H), 1.68-1.44 (m, 10H), 1.43-0.97 (m, 94H), 0.85 (d, *J* = 6.4 Hz, 48H)

^{13}C NMR (126 MHz, $CDCl_3$) δ 138.12, 137.97, 135.94, 135.88, 128.52, 128.42, 128.36, 128.32, 127.84, 127.81, 127.73, 127.64, 127.58, 77.20, 76.57, 76.50, 73.42, 72.22, 70.03, 69.19, 69.16, 68.84, 67.07, 67.00, 66.93, 66.88, 37.52, 37.47, 37.40, 37.38, 36.96, 36.57, 34.29, 33.04, 32.78,

29.85, 29.65, 24.46, 24.37, 19.82, 19.77, 19.72, 19.69. [Multiple signals missing. There are multiple signals with greater intensity suggesting the contribution of multiple nuclei]
^{31}P NMR (162 MHz, $CDCl_3$) -0.86, -0.87. [Two peaks are observed due to diastereomers at phosphorus]
HRMS (ESI+); calculated for $C_{134}H_{224}O_{16}P_2$ $[M+2H]^{2+}$ 1075.8089, found 1075.8094
$[\alpha]_D^{23}$ = +0.87 (c = 0.63, $CHCl_3$)

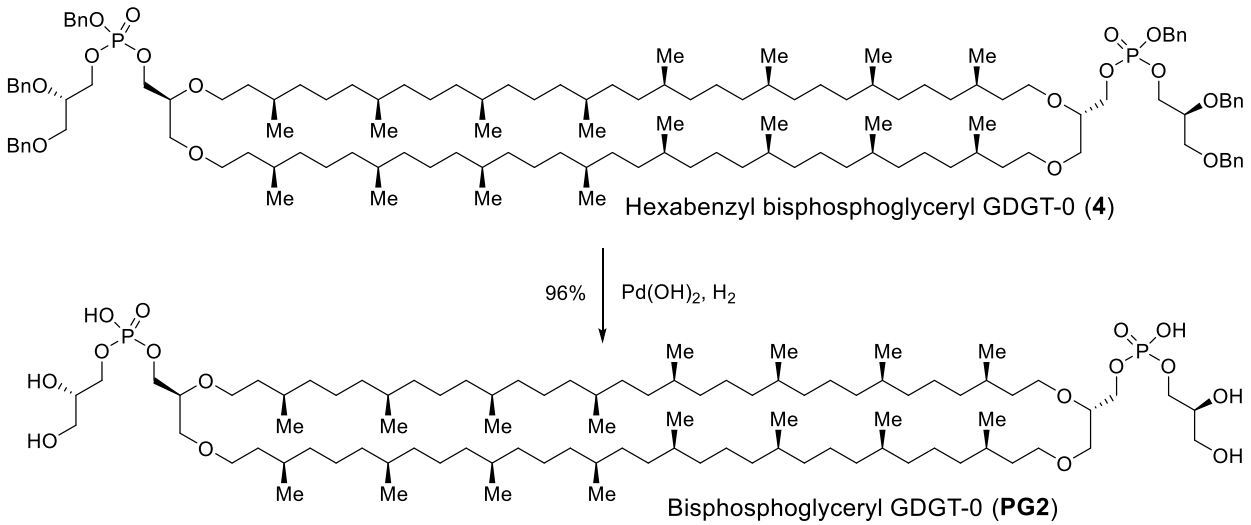

Scheme S5. Reaction scheme for synthesizing bisphosphoglyceryl GDGT-0 (**PG2**).

Bisphosphoglyceryl GDGT-0 (PG2) (Scheme 5): The benzyl-protected phosphate ester **4** (15 mg, 7.0 µmol, 1.0 equiv) was suspended in 1:1 THF/EtOH (2 mL). To the solution was added a small amount of 20% $Pd(OH)_2/C$ (~1 mg, 1.4 µmol, 0.2 equiv). H_2 was bubbled through the solution for 5 min and then the reaction was stirred under an atmosphere of H_2 for ~18 h. The reaction mixture was then passed over celite with CH_2Cl_2 and MeOH and concentrated *in vacuo*. The crude residue was passed over a column of Sephadex LH-20 using 50% MeOH/$CHCl_3$ as the eluent to afford the desired product bisphosphoglyceryl GDGT-0 (**PG2**) (10.8 mg, 96% yield).
Physical Properties: Colourless oil
^{1}H NMR (600 MHz, 1:2 $CDCl_3/CD_3OD$) δ 3.95-3.81 (m, 8H), 3.75 (p, *J* = 5.2 Hz, 2H), 3.71-3.54 (m, 12H), 3.54-3.45 (m, 6H), 1.58 (m, 9H), 1.44-1.16 (m, 74H), 1.09 (m, 27H), 0.87 (m, 48H)
^{13}C NMR (151 MHz,1:2 $CDCl_3/CD_3OD$) ^{13}C NMR (151 MHz, cd_3od) δ 78.72, 71.91, 71.75, 71.75, 70.25, 69.09, 66.77, 65.27, 65.27, 63.11, 63.11, 63.11, 37.88, 37.88, 37.54, 34.72, 34.72, 33.39, 33.39, 33.39, 32.40, 30.24, 30.07, 26.09, 24.93, 24.93, 24.93, 24.93, 23.10, 23.10, 20.11, 18.95, 14.13 δ [^{31}P coupling results in 12 shifts in the range of 60-80 ppm whereas 8 ^{13}C from the α-carbons are expected. Multiple signals are missing. There are multiple signals with greater intensity suggesting the contribution of multiple nuclei]
^{31}P NMR (162 MHz, 1:2 $CDCl_3/CD_3OD$) δ - 0.08
LRMS (ES–) calculated. for $C_{92}H_{185}O_{16}P_2$ $[M-H]^-$ 1608.3, found 1608.8
$[\alpha]_D^{23}$ = **–**3.49 (c = 0.29, 1:1 $CHCl_3$/MeOH)

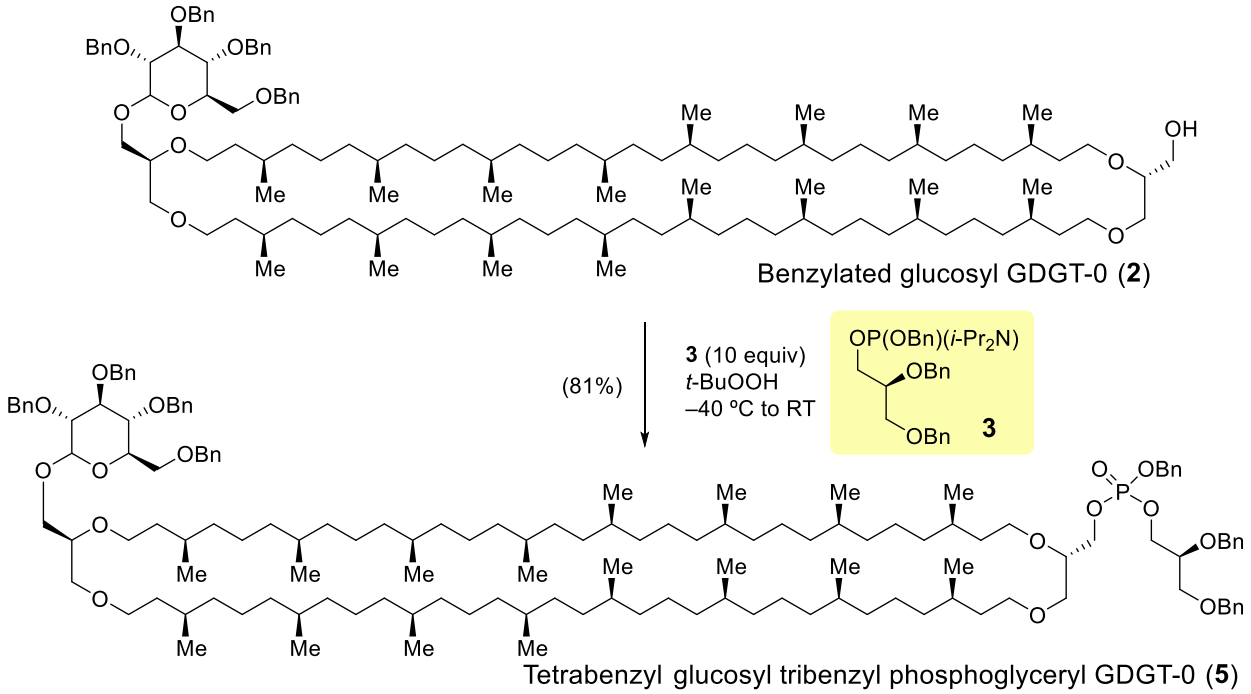

Scheme S6. Reaction scheme for synthesizing tetrabenzyl glucosyl tribenzyl phosphoglyceryl GDGT-0 (**5**).

Tetrabenzyl glucosyl tribenzyl phosphoglyceryl GDGT-0 (5) [Mixture of anomers] (Scheme S6): To a solution of benzylated glucosyl GDGT-0 (**2**) (7.0 mg, 3.8 µmol, 1.0 equiv) in anhydrous CH_2Cl_2 (0.1 mL) in a screw cap vial was added phosphoramidite **3** (20 mg, 38 µmol, 10.0 equiv). To this solution was added 0.45 M solution of tetrazole in acetonitrile (150 µL, 69 µmol, 18 equiv) and the septum was replaced by a screw cap. The reaction was stirred at room temperature for approximately 16 hours. TLC indicated full conversion and to this solution was added a 5.5 M solution of *t*-butyl hydroperoxide in decane (21 µL, 0.12 µmol, 30 equiv). After 20 min, the reaction mixture was directly loaded onto a silica gel preparative TLC plate and purified using 20% EtOAc/hexanes to afford **5** (7.0 mg, 81% Yield, 2:1 ratio of α/β anomers as determined in the next step).

Physical Properties: Colourless oil

^{1}H NMR (600 MHz, $CDCl_3$) δ 7.42-7.23 (m, 33H), 7.15 (m, 2H), 5.06-4.90 (m, 3H), 4.84-4.59 (m, 7H), 4.55-4.42 (m, 4H), 4.24-4.19 (m, 1H), 4.15-4.06 (m, 2H), 4.04-3.94 (m, 2H), 3.84-3.41 (m, 22H), 1.65-1.46 (m, 14H), 1.42-1.15 (m, 64H), 1.14-0.99 (m, 28H), 0.91-0.80 (m, 48H).

^{13}C NMR (101 MHz, $CDCl_3$) δ138.87, 138.62, 138.53, 138.46, 138.39, 138.13, 137.98, 137.95, 135.95, 128.53, 128.44, 128.37, 128.33, 128.31, 128.29, 128.26, 128.12, 127.94, 127.90, 127.87, 127.82, 127.75, 127.71, 127.65, 127.62, 127.59, 127.52, 103.90, 97.31, 84.67, 82.15, 82.00, 80.01, 77.99, 77.77, 77.61, 75.62, 74.98, 74.90, 74.65, 73.44, 72.81, 72.23, 70.92, 70.04, 69.97, 69.16, 68.86, 68.44, 67.83, 67.08, 66.90, 64.25, 37.53, 37.48, 37.39, 37.11, 36.96, 36.69, 36.58, 34.30, 33.05, 32.79, 29.85, 29.73, 29.66, 24.47, 24.38, 19.83, 19.78, 19.73, 19.70. [Multiple signals are missing. There are multiple signals with greater intensity suggesting the contribution of multiple nuclei]

^{31}P NMR (162 MHz, $CDCl_3$) δ -0.87, -0.88

HRMS (ES+) calculated for $C_{144}H_{236}NO_{16}P$ $[M+H+NH_4]^{2+}$ 1133.370550, found 1133.3723

$[\alpha]_D^{23}$ = +4.45 (c = 0.22, $CHCl_3$)

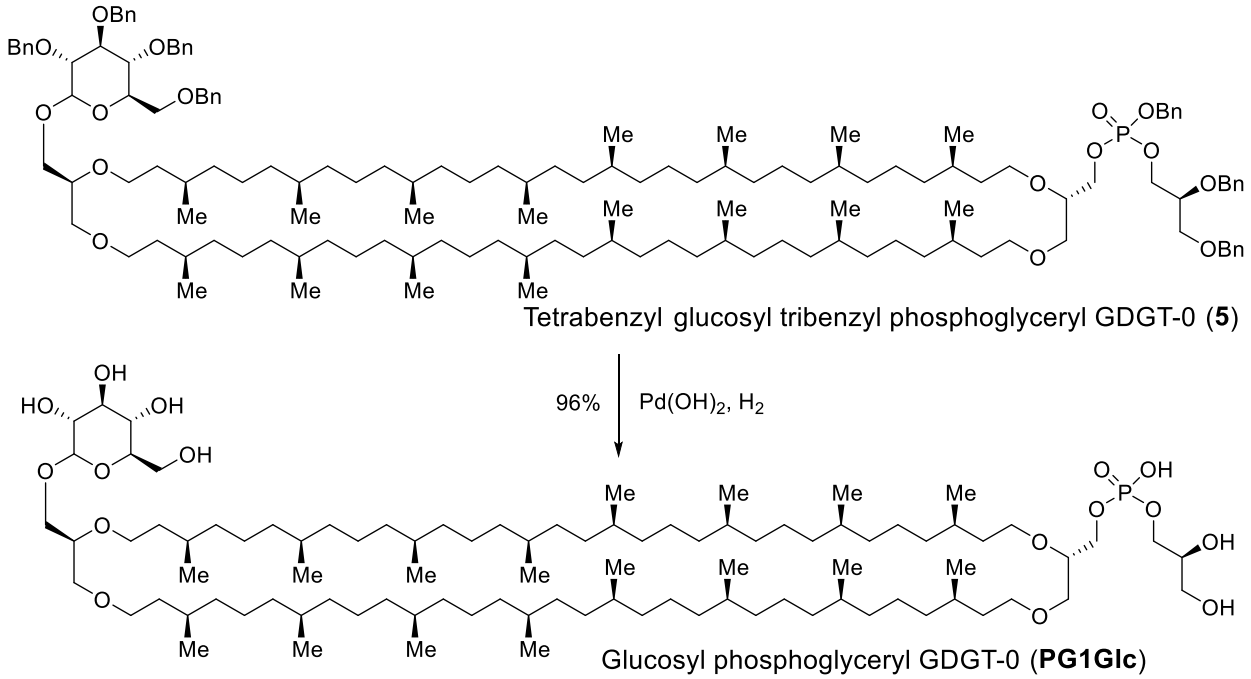

Scheme S7. Reaction scheme for synthesizing bisphosphoglyceryl GDGT-0 (**PG1Glc**).

Glucosyl phosphoglyceryl GDGT-0 (PG1Glc) [Mixture of anomers] (Scheme S7): The benzyl-protected phosphate ester **5** (15 mg, 7.0 μmol, 1.0 equiv) was suspended in a 1:1 mixture of THF/EtOH (2 mL). To the solution was added a small amount of 20% $Pd(OH)_2/C$ (~1 mg, 1.4 μmol, 0.2 equiv). H_2 was bubbled through the solution for 5 min and then the reaction was stirred under an atmosphere of H_2 for ~18 h. The reaction mixture was then passed over celite with CH_2Cl_2 and MeOH and concentrated *in vacuo*. The crude residue was passed over a column of Sephadex LH-20 using 50% MeOH/$CHCl_3$ as the eluent to afford the desired product **PG1Glc** (10.8 mg, 96% Yield, 2:1 ratio of α/β anomers).

Physical Properties: Colourless oil

^{1}H NMR (600 MHz, 1:1 $CDCl_3/CD_3OD$) δ 4.78 (d, *J* = 3.7 Hz, 0.60H, α-anomer), 4.26 (d, *J* = 7.7 Hz, 0.30H, β-anomer), 4.10-3.34 (m, 29H), 1.63-1.49 (m, 9H), 1.42-1.16 (m, 74H), 1.07 (m, 28H), 0.91-0.78 (m, 48H)

^{13}C NMR (151 MHz, 1:1 $CDCl_3/CD_3OD$) δ 103.79, 99.31, 78.22, 76.73, 76.56, 74.40, 74.40, 73.90, 72.74, 72.58, 72.41, 71.41, 71.08, 70.58, 70.25, 69.26, 69.09, 67.60, 67.43, 66.60, 65.77, 65.27, 63.61, 63.28, 61.95, 61.78, 61.62, 37.71, 37.54, 37.05, 34.56, 34.39, 33.06, 32.06, 30.07, 29.74, 25.76, 24.76, 24.76, 24.59, 24.59, 22.77, 22.77, 21.94, 19.94, 19.78, 18.95, 13.97 [Multiple signals are missing. There are multiple signals with greater intensity suggesting the contribution of multiple nuclei]

^{31}P NMR (162 MHz, 1:1 $CDCl_3/CD_3OD$) δ 0.56

HRMS (ES–) calc. For $C_{95}H_{188}O_{16}P$ $[M\text{-}H]^-$ 1616.3635, found 1616.3661

$[\alpha]_D^{23}$ = +3.65 (c = 0.195, 1:1 MeOH/$CHCl_3$)

Fitting of SAXS data from unilamellar vesicles

The buffer-subtracted and averaged data were fit using the model for unilamellar vesicles,[3] which is based on approximating the electron density of the bilayer by three Gaussian peaks corresponding to the inner and outer phosphate peak and a negative trough at the centre. The following equation was used for the fits:

$$I(q) = I_0 q^{-2} \sum_{i,j}^{n=3} (R_0 + \epsilon_i)\left(R_0 + \epsilon_j\right)\rho_i\rho_j\sigma_i\sigma_j \exp[-q^{-2}\left(\sigma_i^2 + \sigma_j^2\right)/2]\cos\left[q(\epsilon_i - \epsilon_j)\right] + a_0 + a_1 q \ldots (1)$$

where,

I_0: overall intensity of the measured profile

R_0: mean radius of the vesicle measured at the centre of the bilayer

ε: peak displacements from the bilayer centre

σ: Gaussian width of the peak

ρ: amplitude of the peak

a_0: constant background term

a_1: linear background term

The measured data were fit over the range q = 0.02 – 0.65 Å^{-1}. Data fitting was carried out based on a simulated annealing algorithm and the results were then further optimized using a non-linear least square algorithm, by using code from the open-source GNU scientific library project (https://www.gnu.org/software/gsl/). The fit parameters are summarized in Table S1.

Table S1: Fitting parameters of SAXS intensity profiles of GDGT lipids (Fig. 5A) that were used to generate the corresponding electron density profiles (Fig. 5B) according to Equation 1. The bilayer centre (ε_2) was fixed at 0. The head-to-head distances of the lipids in a membrane (d) are calculated as a difference between positions of peak maxima of the 1st (ε_1) and 3rd (ε_3) gaussians.

Lipid	ρ_1	ε_1 (Å)	σ_1 (Å)	ρ_2	σ_2 (Å)	ρ_3	ε_3 (Å)	σ_3 (Å)	I_0 (×10^{-7})	R_0 (Å)	a_0	a_1	χ^2/DOF	d = ε_3 - ε_1 (Å)
P2	1.98 ± 0.04	-19.0 ± 0.38	4.57 ± 0.09	-0.84 ± 0.02	10.7 ± 0.22	4.77 ± 0.10	20.8 ± 0.42	1.00 ± 0.02	5.12 ± 0.10	55.9 ± 1.00	0.29 ± 0.01	0.13 ± 0.00	0.08	39.8 ± 0.80
P1Glc	1.41 ± 0.03	-22.7 ± 0.44	5.00 ± 0.10	-0.84 ± 0.02	11.7 ± 0.24	7.41 ± 0.16	16.4 ± 0.34	0.90 ± 0.02	0.35 ± 0.01	47.6 ± 1.00	0.12 ± 0.00	0.00 ± 0.00	0.01	39.1 ± 0.78
PG2	0.88 ± 0.02	-17.4 ± 0.38	5.40 ± 0.10	-0.60 ± 0.02	10.7 ± 0.20	2.11 ± 0.03	21.3 ± 0.40	1.58 ± 0.01	5.27 ± 0.10	77.8 ± 1.00	0.71 ± 0.01	0.13 ± 0.00	0.08	38.7 ± 0.78
PG1Glc	1.53 ± 0.03	-18.3 ± 0.36	5.01 ± 0.10	-0.99 ± 0.02	10.7 ± 0.22	3.55 ± 0.06	20.2 ± 0.42	1.59 ± 0.04	1.15 ± 0.02	57.1 ± 1.00	0.22 ± 0.00	0.01 ± 0.00	0.01	38.5 ± 0.78

Supplementary Figures

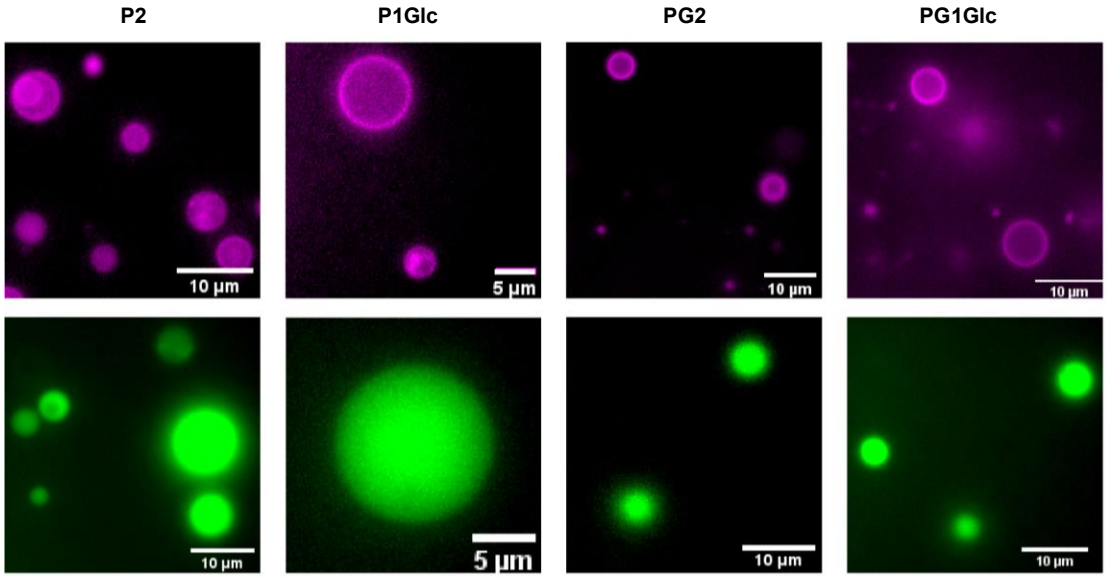

Fig. S1 Microscopy images of giant vesicles of GDGT lipids formed by gentle hydration of a thin lipid film in Tris buffer (50 mM, pH 7.5). *Upper panel*: membranes are stained by the lipophilic dye Texas Red-DHPE incorporated at 0.1 mol%. *Lower panel*: encapsulation of water-soluble dye pyranine (0.5 mM) in the interior of vesicles.

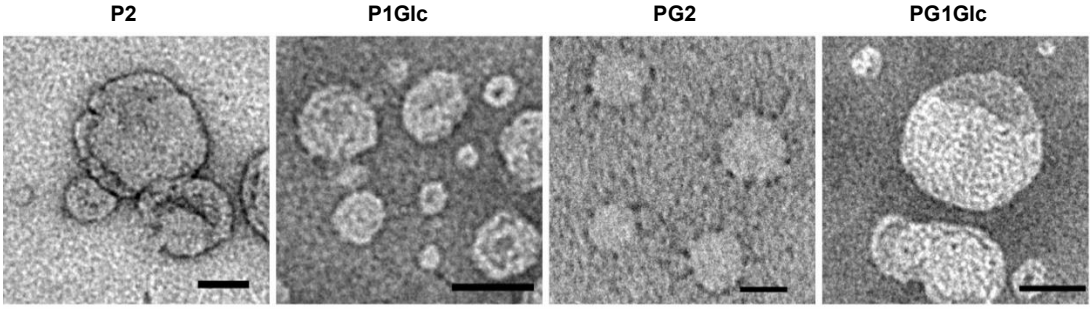

Fig. S2 Negative-staining electron microscopy images of vesicles of GDGT lipids obtained via extrusion (**P2**, **PG2**, **PG1Glc**) or ultrasonication (**P1Glc**) of multilamellar dispersions. All scale bars correspond to 50 nm.

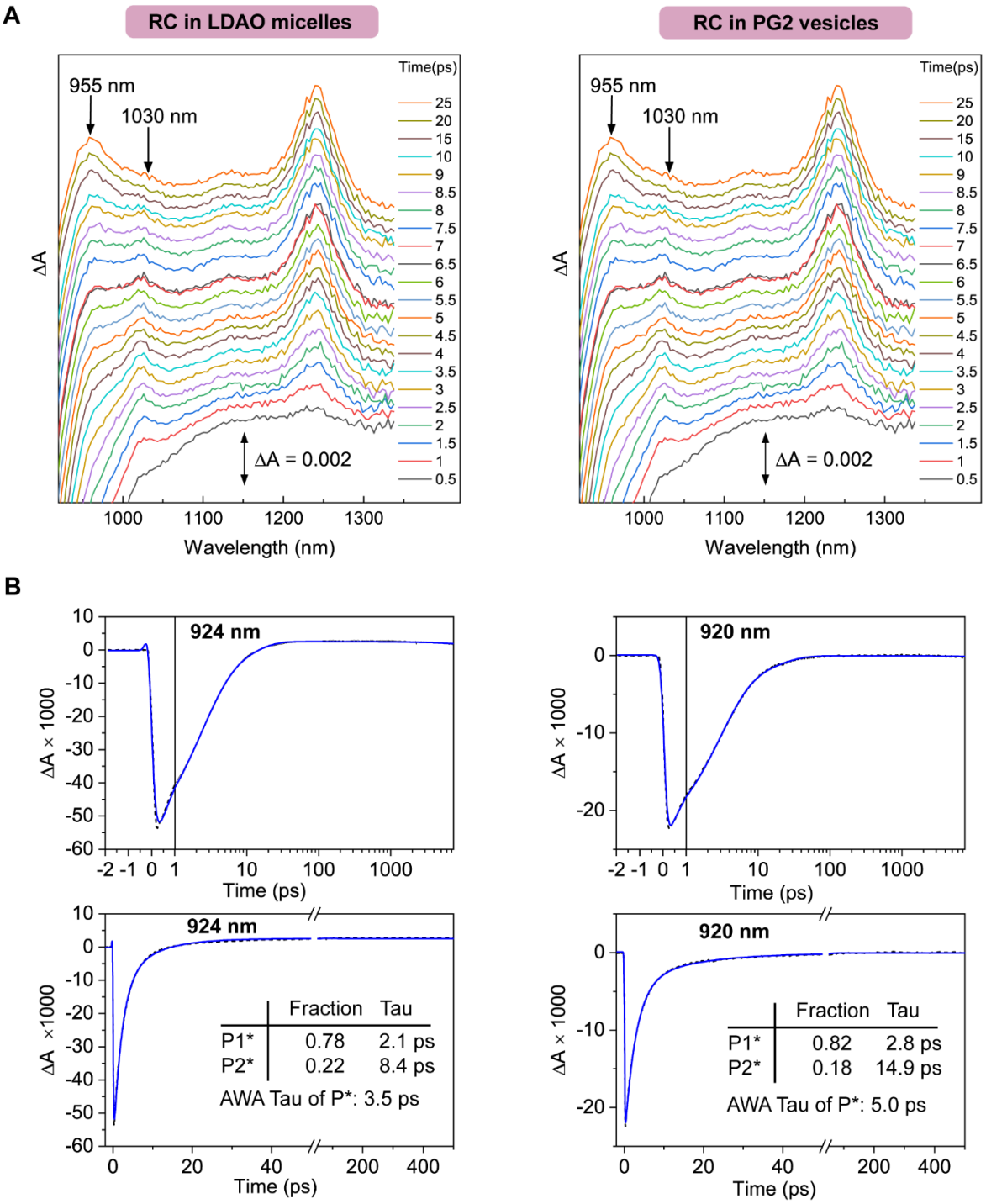

Fig. S3 Ultrafast transient absorption spectroscopy of bacterial (*Rhodobacter spheroides*) photosynthetic reaction centres (M252V mutant which assembles without Q_A) in archaeal lipid vesicles at 295 K. **A**. Time evolution of the near IR spectra at 0.5-25 ps. In both panels, there is a clear band around 1030 nm, which is characteristic of B_A^-, the primary charge transfer intermediate in RC. The difference in signal intensity is most likely due to the difference in concentration. **B**. The two panels show single wavelength kinetics fit at 920 nm for P* stimulated emission decay characterized by the lifetime tau. As P* → $P^+B_A^-$, the decay of P* corresponds to

the formation of B_A^-, hence giving the kinetics of the primary charge transfer process. The lifetimes of the two P* populations in both samples as well as the amplitude-weighted-average (AWA) lifetime are very similar between two samples, indicating that reconstitution into archaeal lipid had negligible effects on the charge transfer process of the RC.

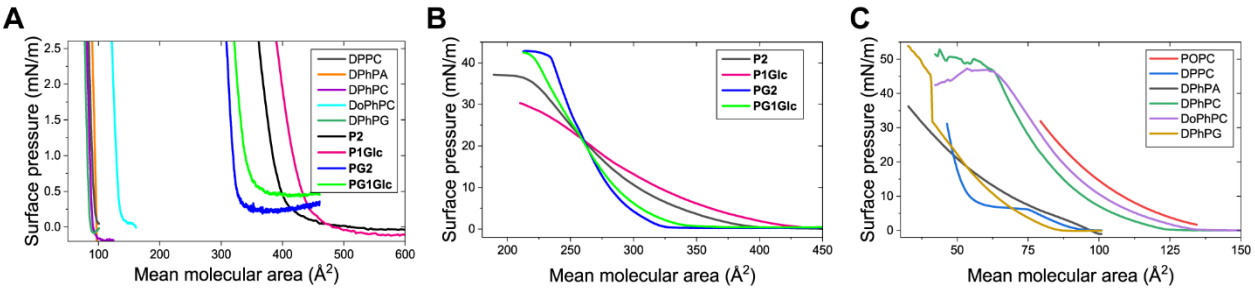

Fig. S4 Expanded plots of surface pressure-area (π-A) isotherms of GDGTs and other lipids. **A**. Lift-off areas (A_0) were calculated by extrapolating the linear regions of the isotherms in the range of surface pressure (π) = 0.5-2.5 mN/m to zero surface pressure. **B**. Zoomed in plot of the π-A isotherms of bipolar lipids described in this study. **C**. Zoomed in plot of the π-A isotherms of the monopolar lipids described in this study.

A

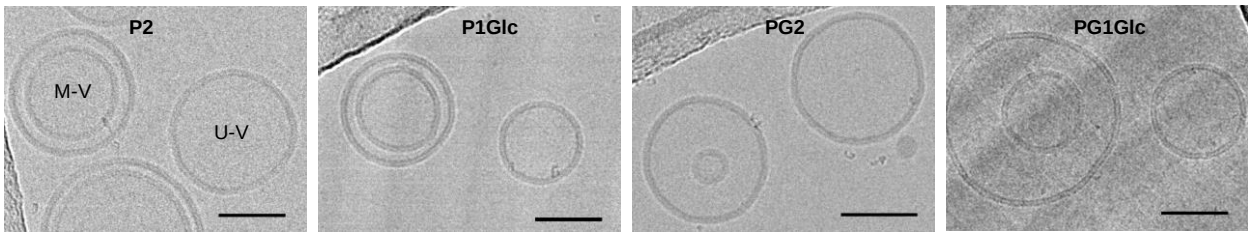

B

Lipid	Uni-vesicular (U-V) %	Multi-vesicular (M-V) %
P2 (67)	36	64
P1Glc (29)	76	24
PG2 (53)	58	42
PG1Glc (51)	76	24

C

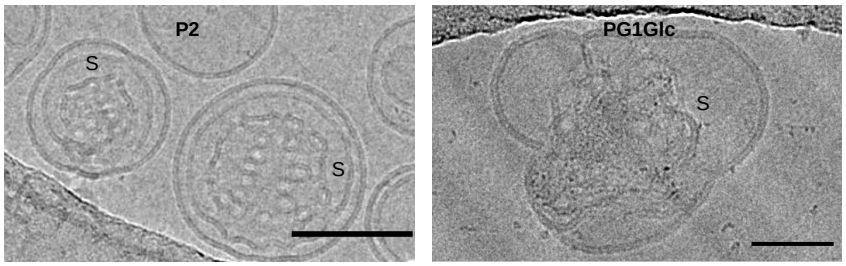

Fig. S5 Cryogenic electron microscopy images of vesicles and other lipidic structures of GDGTs formed in Tris buffer (50 mM, pH 7.5). **A**. Images of unilamellar vesicles: U-V and M-V denote uni-vesicular and multi-vesicular architectures. **B**. Percentages of uni-vesicular and multi-vesicular structures imaged for each lipid. The numbers in parentheses indicate the number of vesicles analysed. **C**. Example of sponge-like structures (denoted by 'S') observed in vesicles of **P2** and **PG1Glc**. All scale bars represent 50 nm.

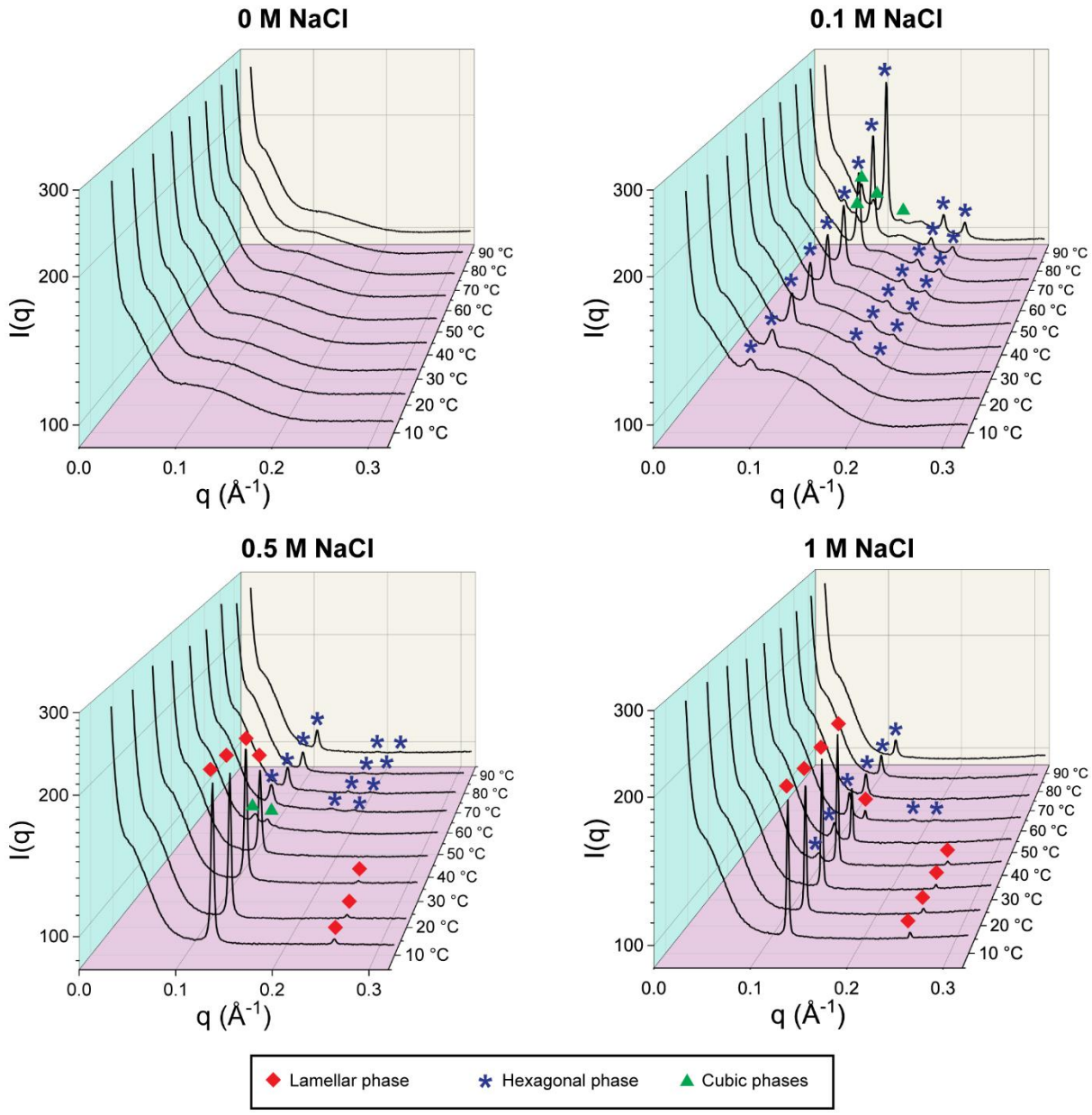

Fig. S6 SAXS intensity profiles of bulk dispersions of **P2** in Tris buffer (50 mM, pH 7.5) containing variable concentrations of salt (NaCl) over 10-90 °C.

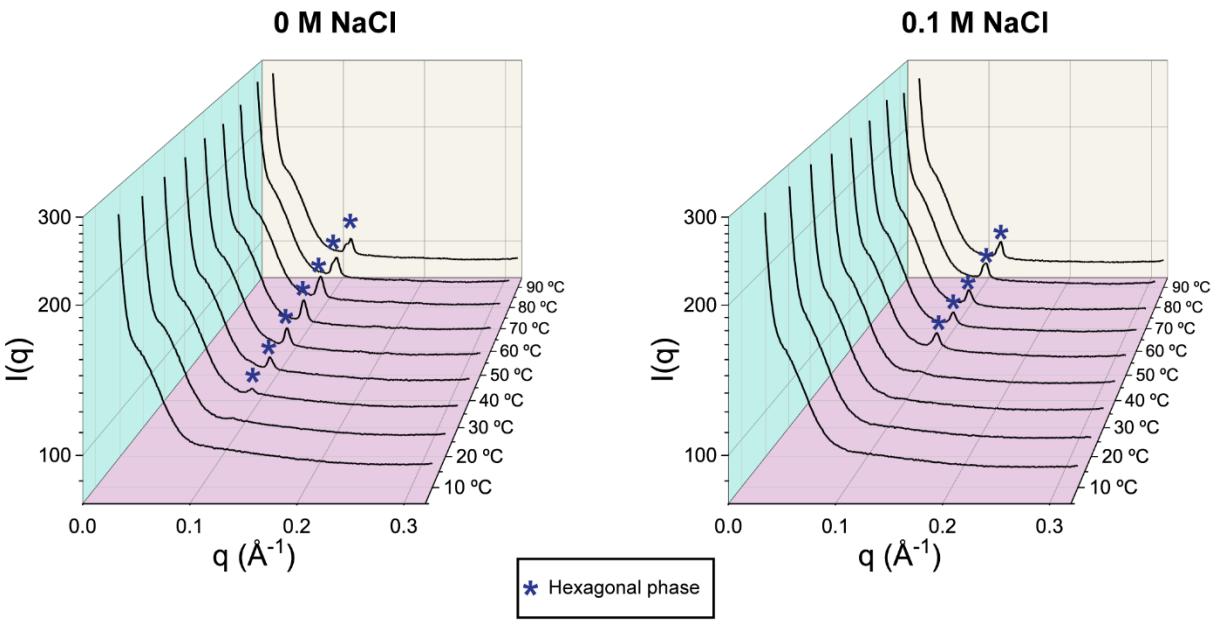

Fig. S7 SAXS intensity profiles of bulk dispersions of **P1Glc** in Tris buffer (50 mM, pH 7.5) containing variable concentrations of salt (NaCl) over 10-90 °C. The lipid films could not be dispersed at salt concentrations above 0.1 M NaCl.

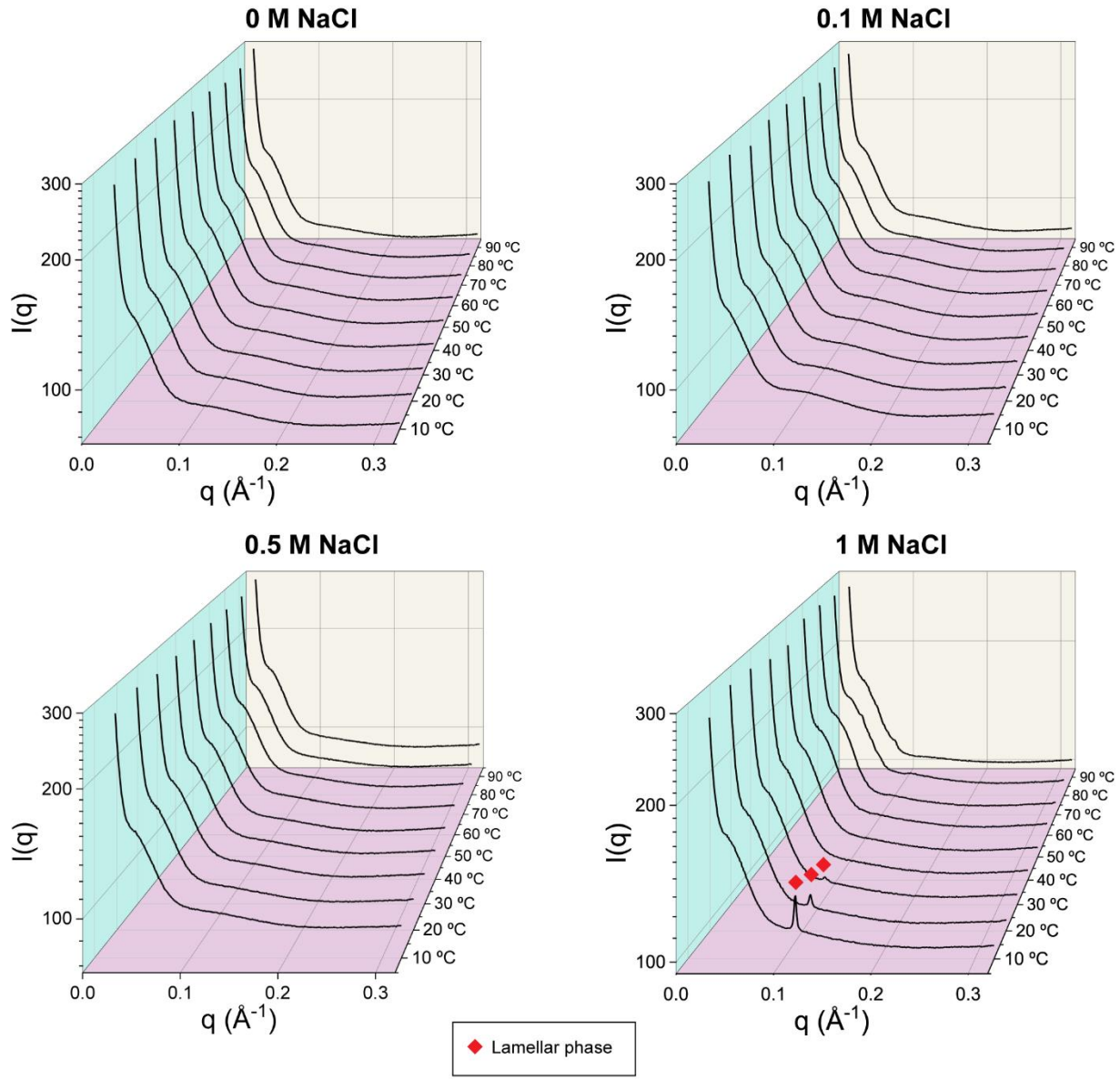

Fig. S8 SAXS intensity profiles of bulk dispersions of **PG2** in Tris buffer (50 mM, pH 7.5) containing variable concentrations of salt (NaCl) over 10-90 °C.

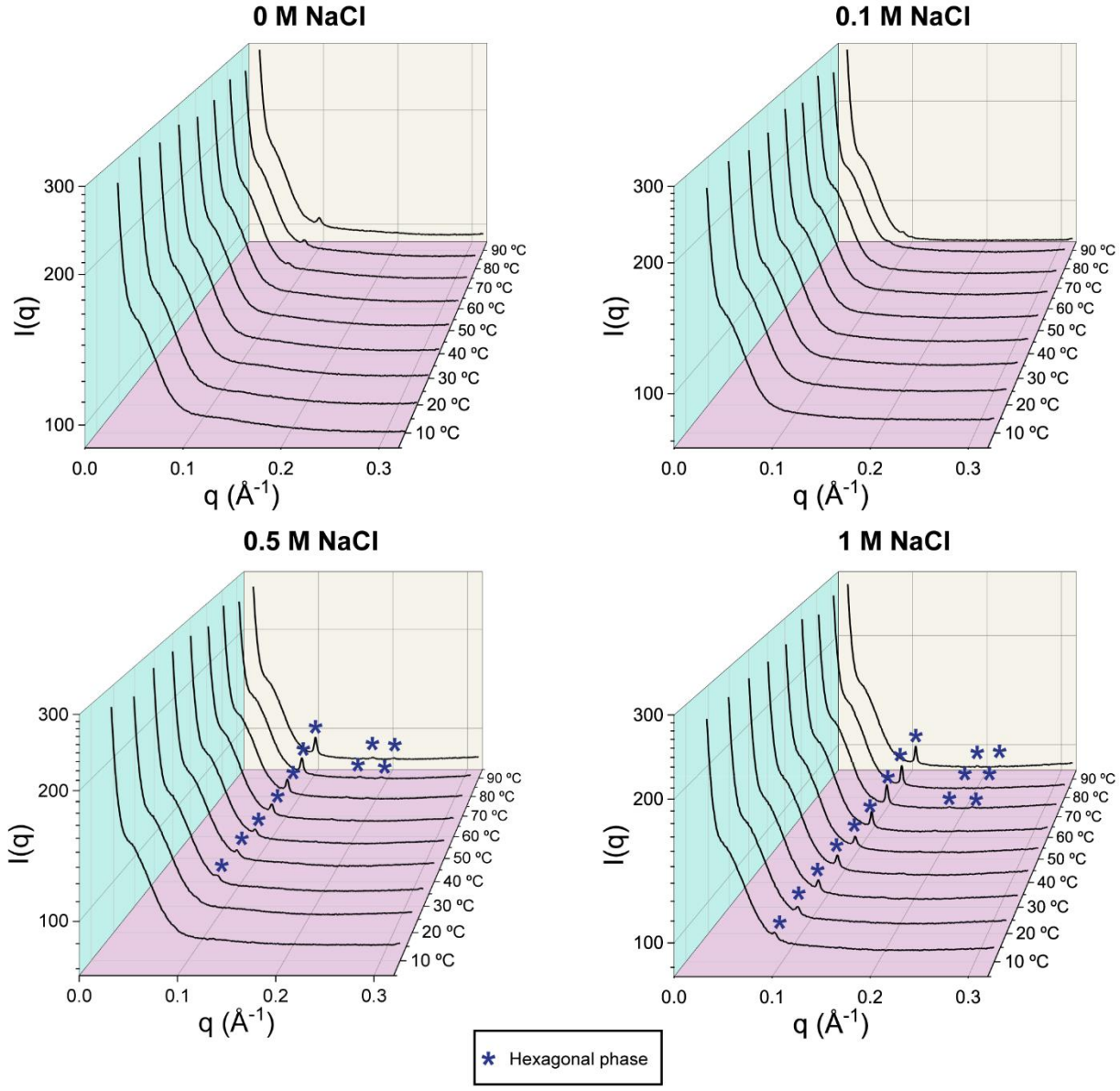

Fig. S9 SAXS intensity profiles of bulk dispersions of **PG1Glc** in Tris buffer (50 mM, pH 7.5) containing variable concentrations of salt (NaCl) over 10-90 °C.

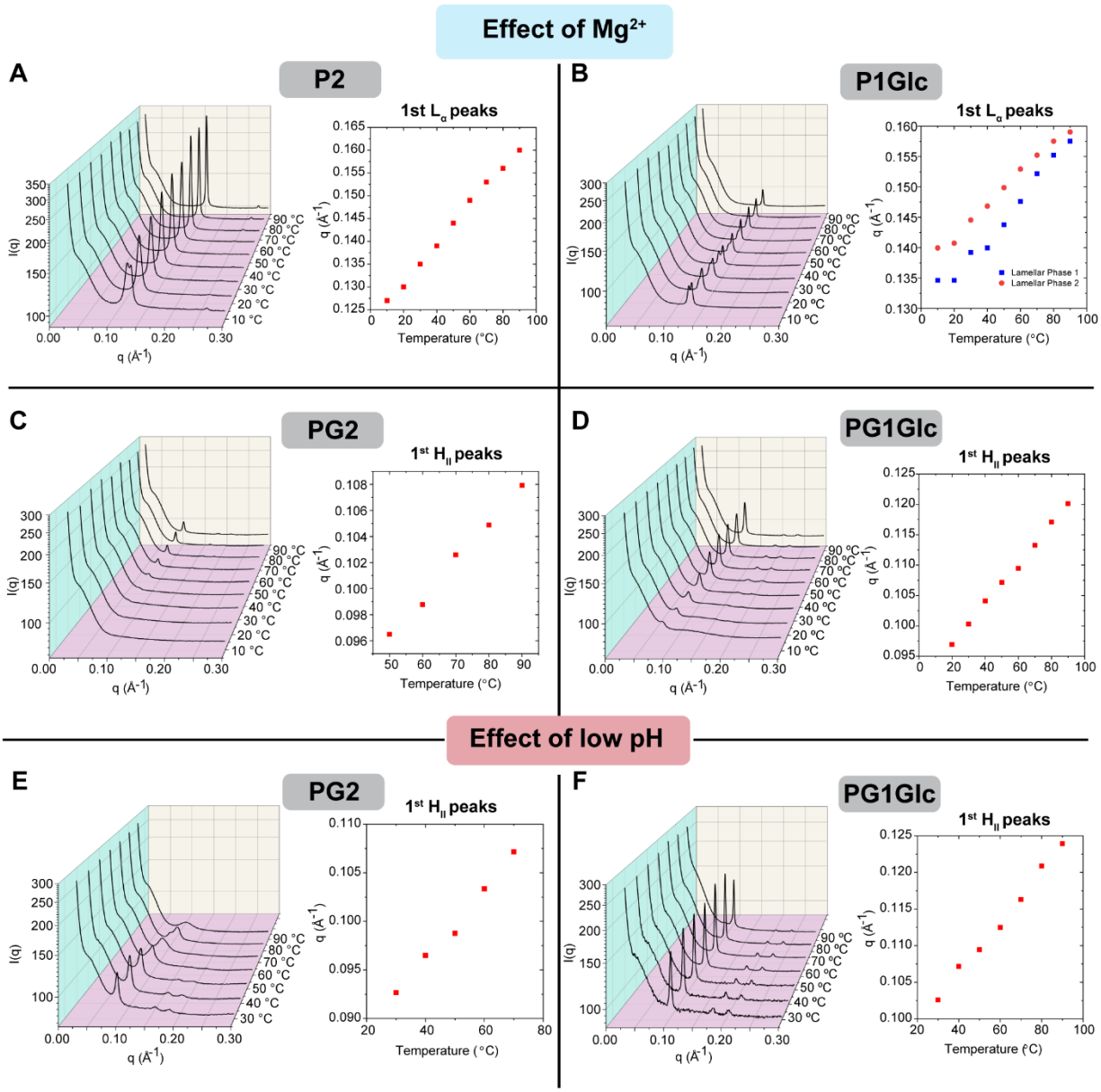

Fig. S10 Small-angle X-ray scattering (SAXS) on bulk dispersions of GDGT lipids in presence of magnesium ions ($MgCl_2$) (**A**, **B**, **C**, **D**) over 10-90 °C and low pH (2.8) (**E**, **F**) over 30-90 °C. Lipidic mesophases such as lamellar (L_α, 1:2:3:4) and inverse hexagonal (H_{II}, 1:√3:√4) were identified from the characteristic ratios of the q-values of the Bragg peaks in the intensity profiles. In all cases, the peak positions (q-value) of the 1st characteristic mesophase peak were found to increase with temperature, likely due to increasing dehydration.

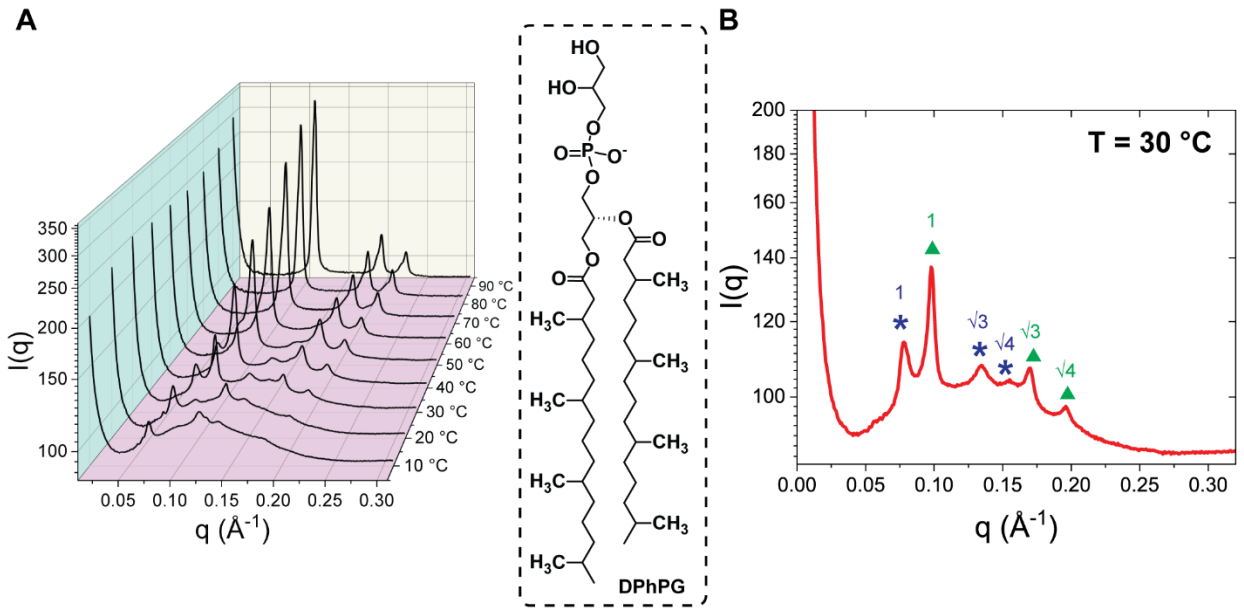

Fig. S11 Mg^{2+}-induced mesophase formation in DPhPG. **A**. SAXS intensity profiles of DPhPG dispersed in Tris buffer (pH 7.5) containing 10 mM Mg^{2+} over 10-90 °C. **B**. The intensity profile for 30 °C is shown in enlarged form to show co-existence of two sets of hexagonal phase peaks (at ratio of 1:√3:√4) – indicated by asterisk (*) and triangles (▲).

100 mol% mix	DPhPG:GD1a:Biotin-DPPE:Atto 47N-DMPE (99.45:0.4:0.1:0.05)
1 mol% mix	**PG2**:DPhPG:GD1a:Biotin-DPPE:Atto 647N-DMPE (99:0.5:0.4:0.1:0.05)
0.5 mol% mix	**PG2**:GD1a:Biotin-DPPE:Atto 647N-DMPE (99.45:0.4:0.1:0.05)

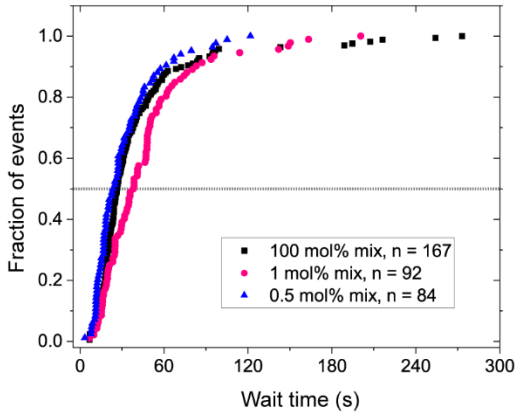

Fig. S12 Acidic pH-induced fusion of influenza virus particles with 100 nm vesicles containing varying mol percentages of monopolar lipids (100, 1, 0.5). The virus was labelled with self-quenching concentration of Texas Red-DHPE, and the vesicle lipid compositions are indicated. Cumulative distribution functions corresponding to wait times to individual lipid mixing events for viral fusion with vesicles are shown. It is notable that the “100 mol% mix” sample has also been referred to as “DPhPG mix” in the main text.

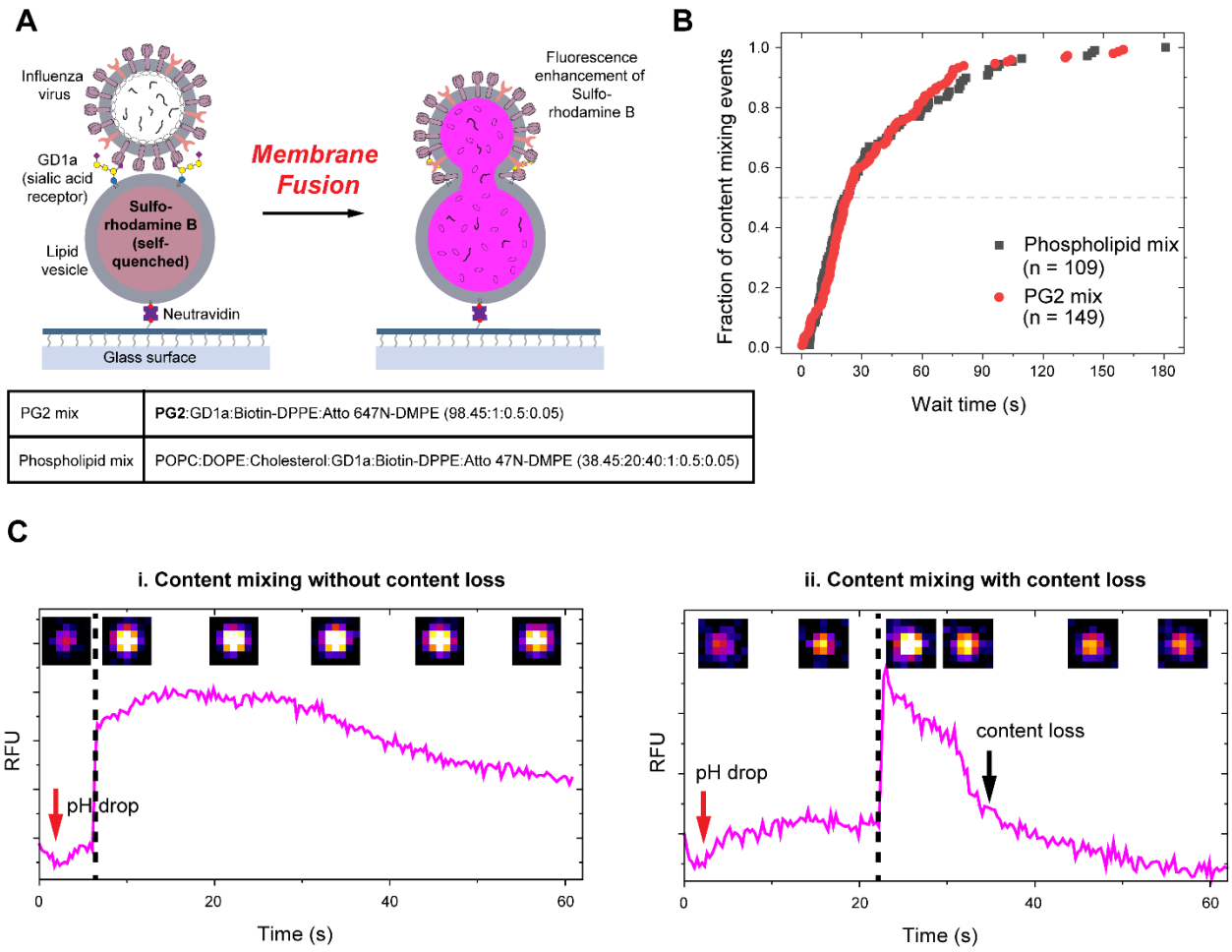

PG2 mix	**PG2**:GD1a:Biotin-DPPE:Atto 647N-DMPE (98.45:1:0.5:0.05)
Phospholipid mix	POPC:DOPE:Cholesterol:GD1a:Biotin-DPPE:Atto 47N-DMPE (38.45:20:40:1:0.5:0.05)

Fig. S13 A. Schematic diagram illustrating content mixing upon fusion of virus particles to tethered lipid vesicles as evident from increase in fluorescence signal of sulforhodamine B dye. **B**. Cumulative distribution functions corresponding to wait times for content transfer events during viral fusion with 100 nm vesicles composed of bipolar lipids ("PG2 mix") and monopolar lipids ("Phospholipid mix"). **C**. Representative fluorescence intensity traces for fusion of "PG2 mix" vesicles with influenza virus particles corresponding to two kinds of events observed: (i) content mixing without any loss (ii) content mixing with content loss.

Supplementary References

(1) Shaw, M.; Kumar, A. Visible-Light-Mediated *β*-C(sp^3)-H Amination of Glycosylimidates: En Route to Oxazoline-Fused/Spiro Nonclassical Bicyclic Sugars. *Org. Lett.* **2019**, *21* (9), 3108–3113.

(2) Eguchi, T.; Arakawa, K.; Kakinuma, K.; Rapp, G.; Ghosh, S.; Nakatani, Y.; Ourisson, G. Giant Vesicles from 72-Membered Macrocyclic Archæal Phospholipid Analogues: Initiation of Vesicle Formation by Molecular Recognition between Membrane Components. *Chem. - A Eur. J.* **2000**, *6* (18), 3351–3358.

(3) Brzustowicz, M. R.; Brunger, A. T. X-Ray Scattering from Unilamellar Lipid Vesicles. *J. Appl. Crystallogr.* **2005**, *38* (1), 126–131.

NMR Spectra

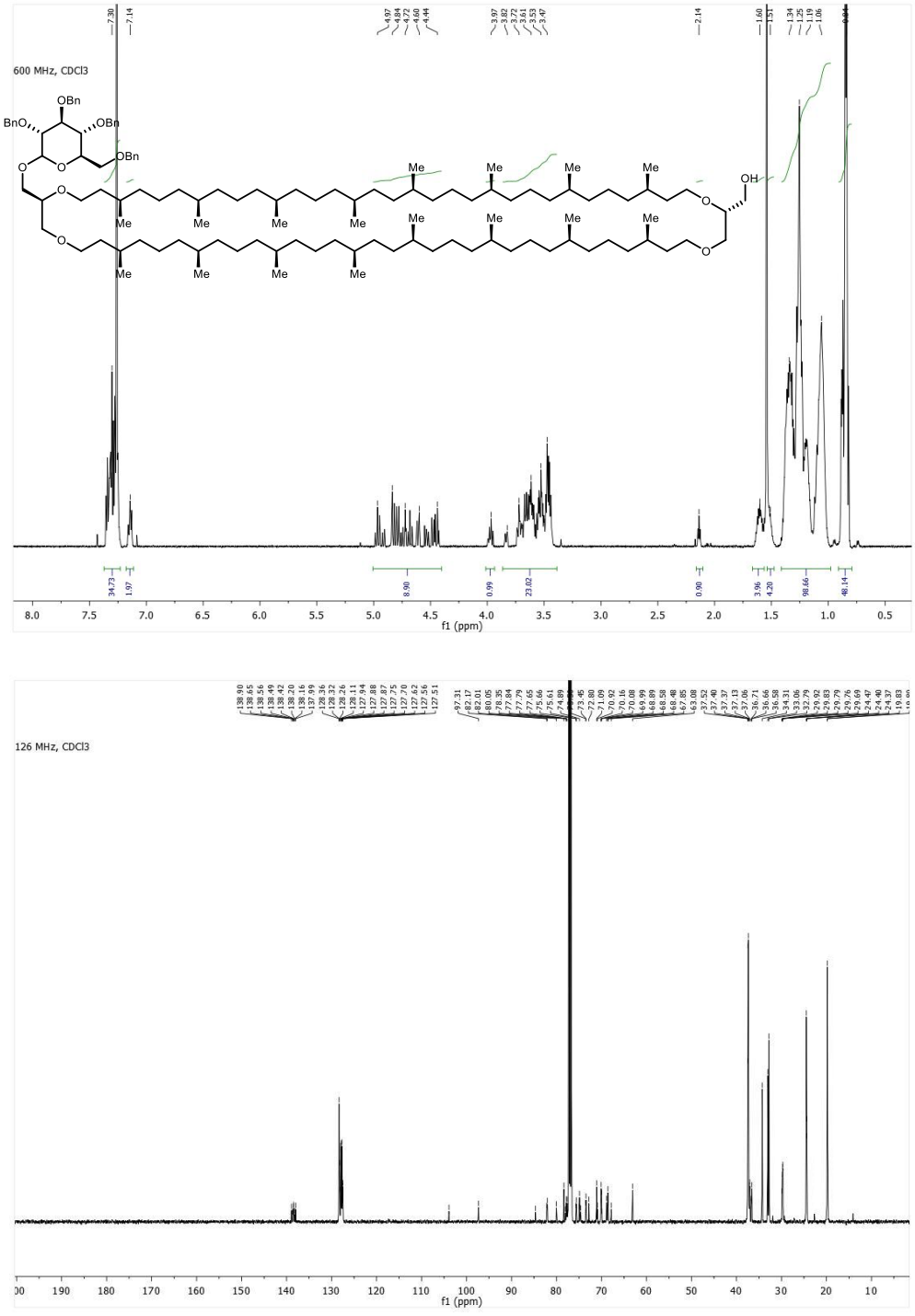

^{1}H NMR (*top*) and ^{13}C NMR (*bottom*) spectra of compound **2**.

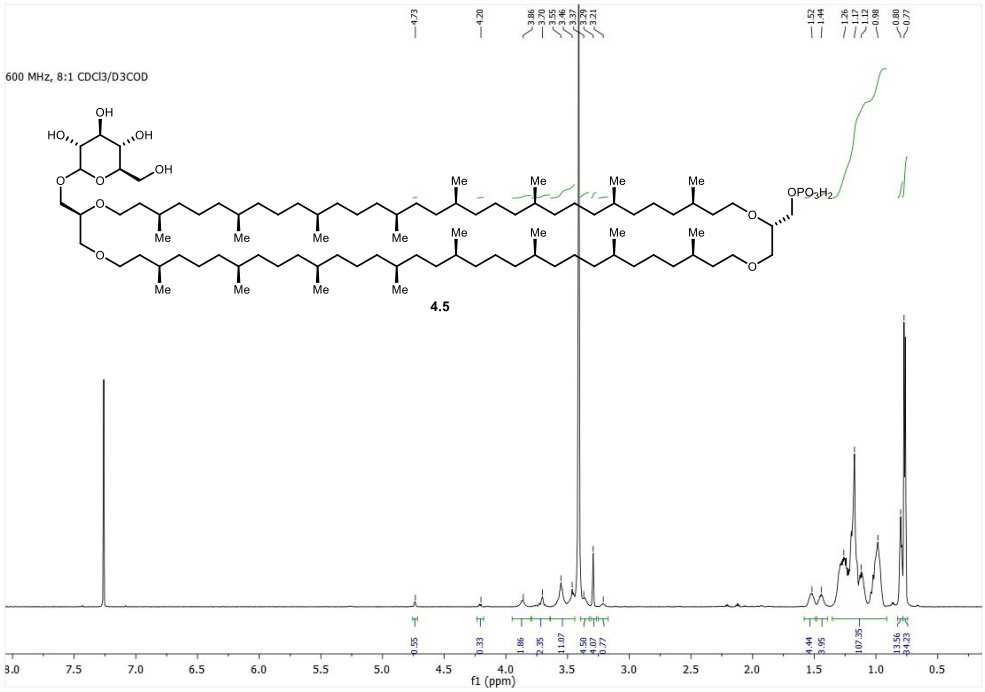

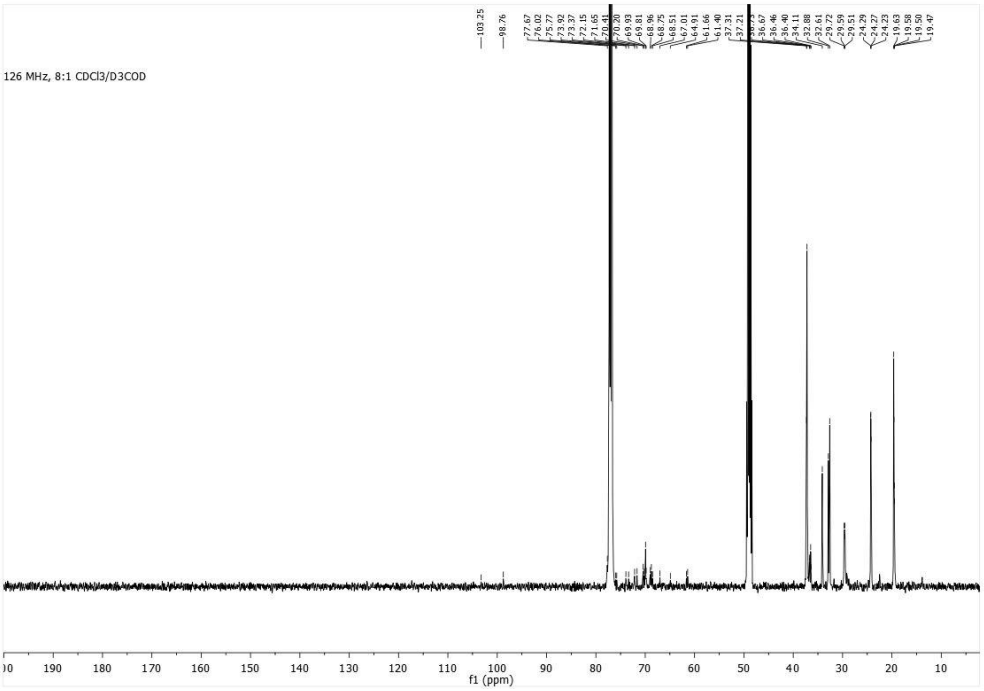

^{1}H NMR (*top*) and ^{13}C NMR (*bottom*) spectra of compound **P1Glc**.

HSQC Data for **P1Glc**:

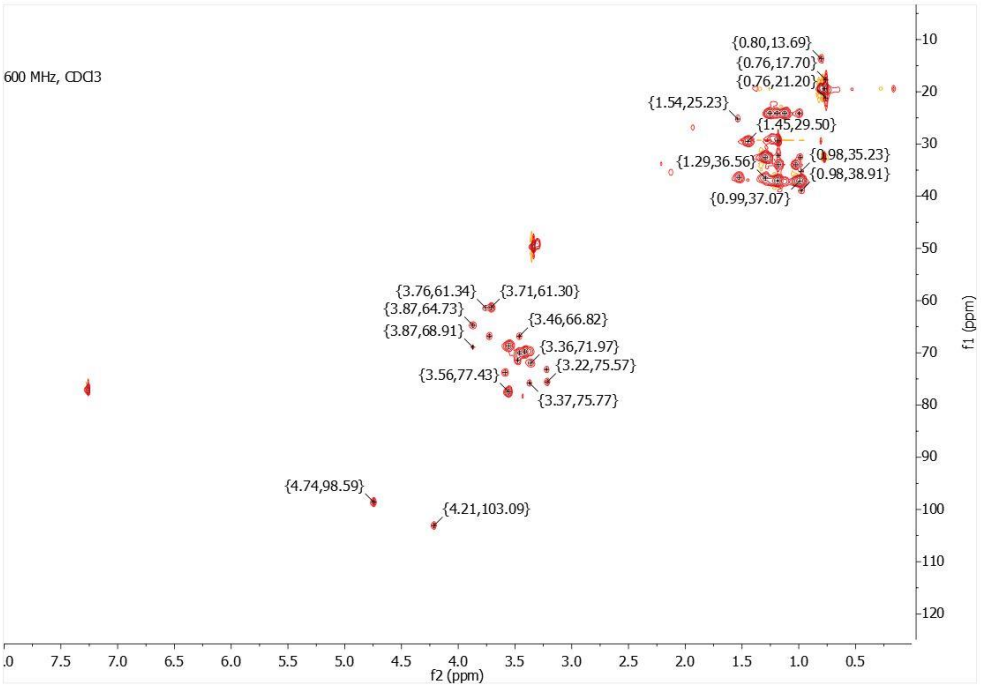

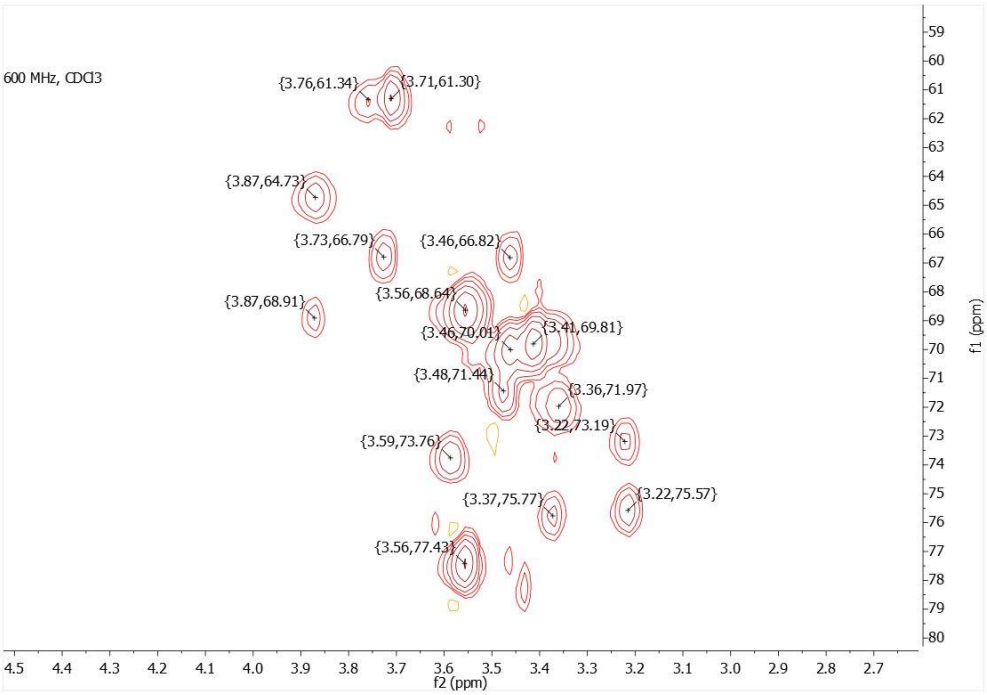

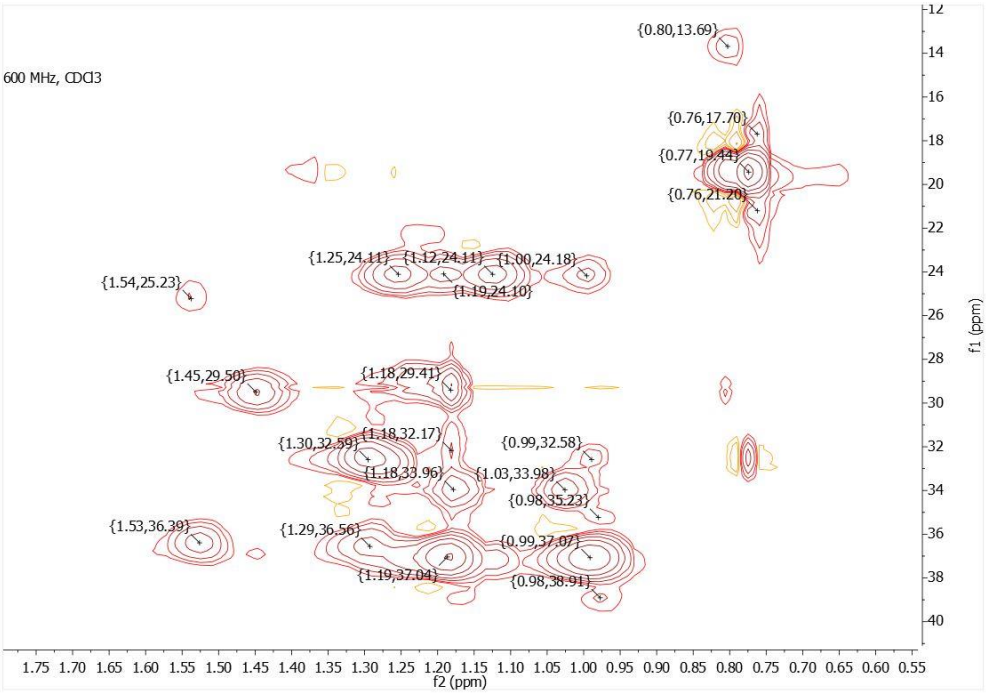

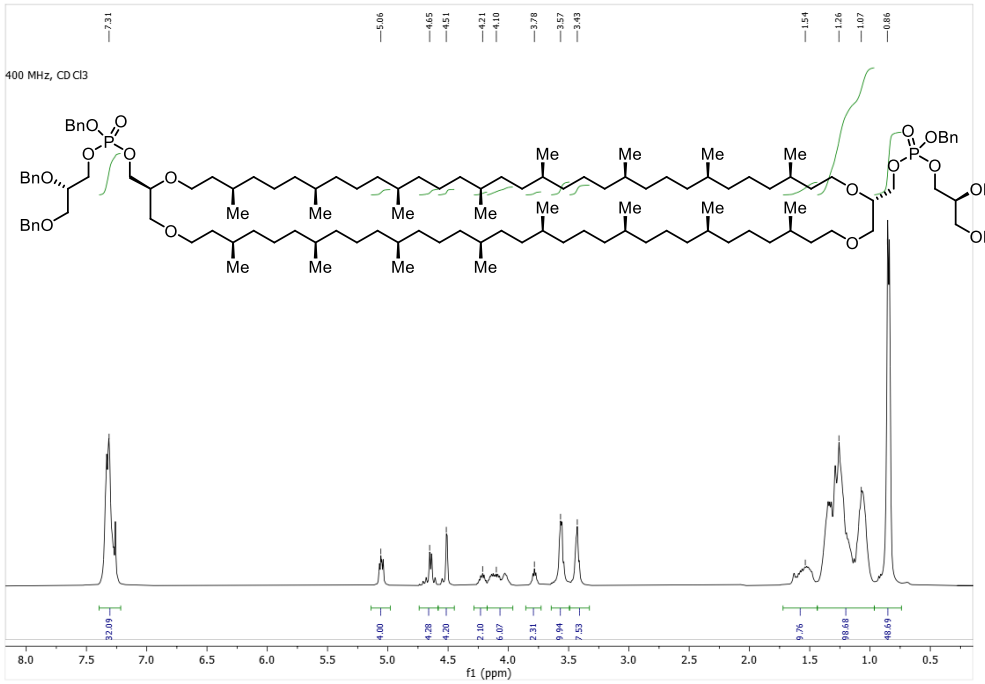

^{1}H NMR spectrum of compound **4.**

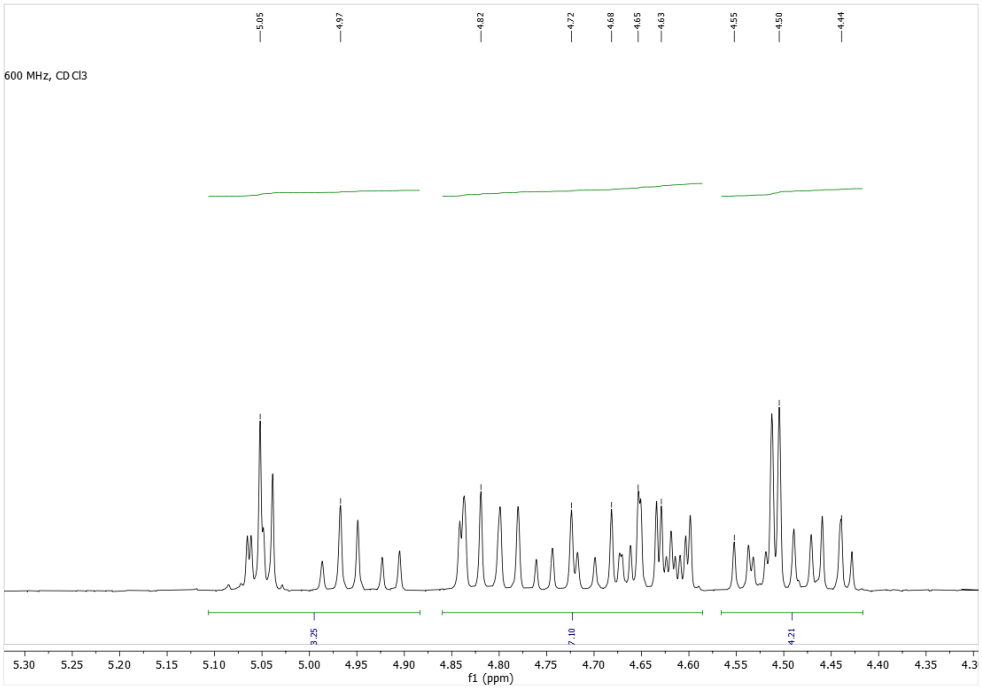

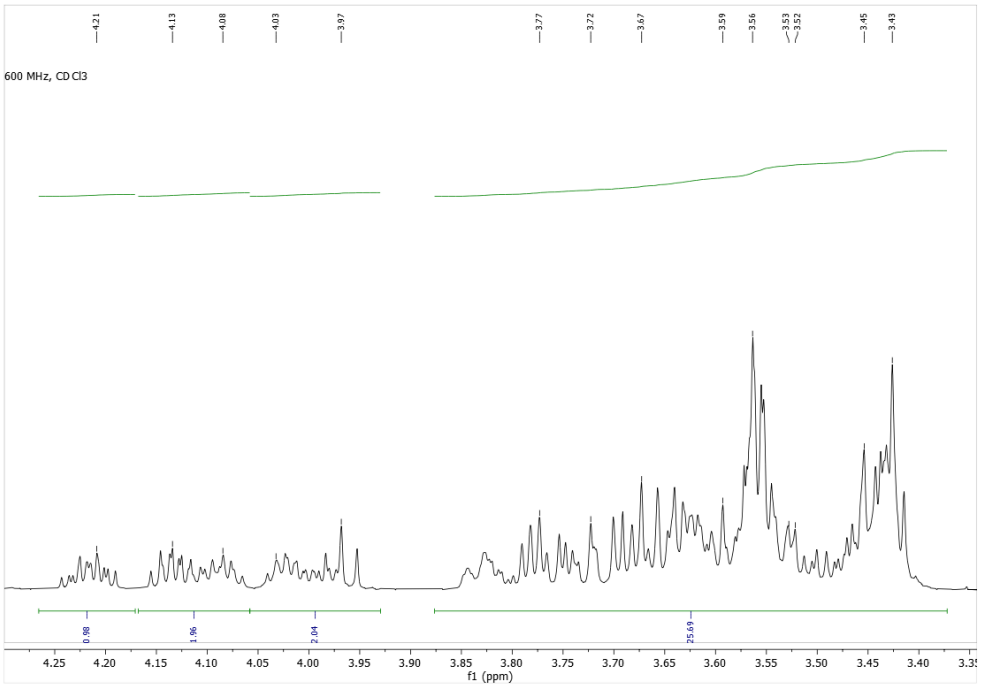

A zoomed in view of the ^{1}H NMR spectrum of compound **4** over δ 5.30-4.30 ppm (*top*) and δ 4.30-3.30 ppm (*bottom*) regions respectively.

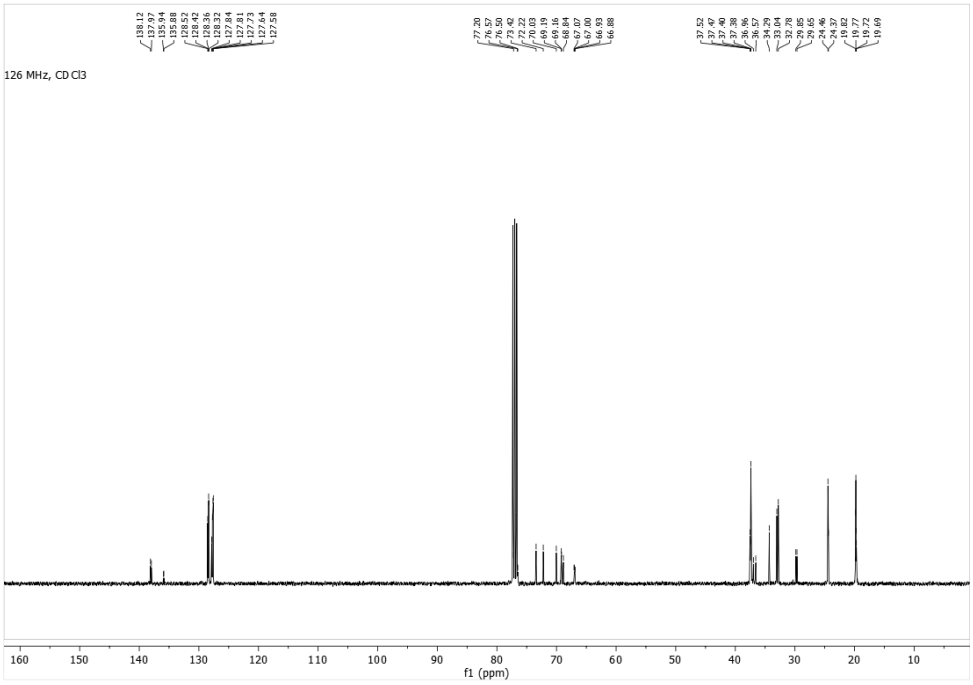

^{13}C NMR spectrum of compound **4**.

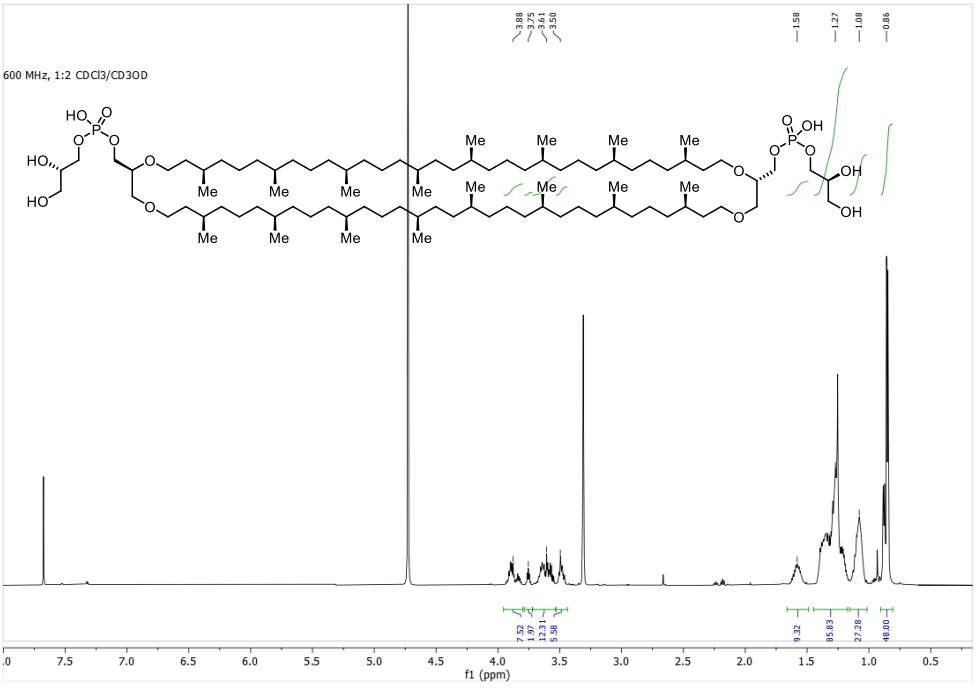

^{1}H NMR spectrum of compound **PG2.**

HSQC Data for **PG2**:

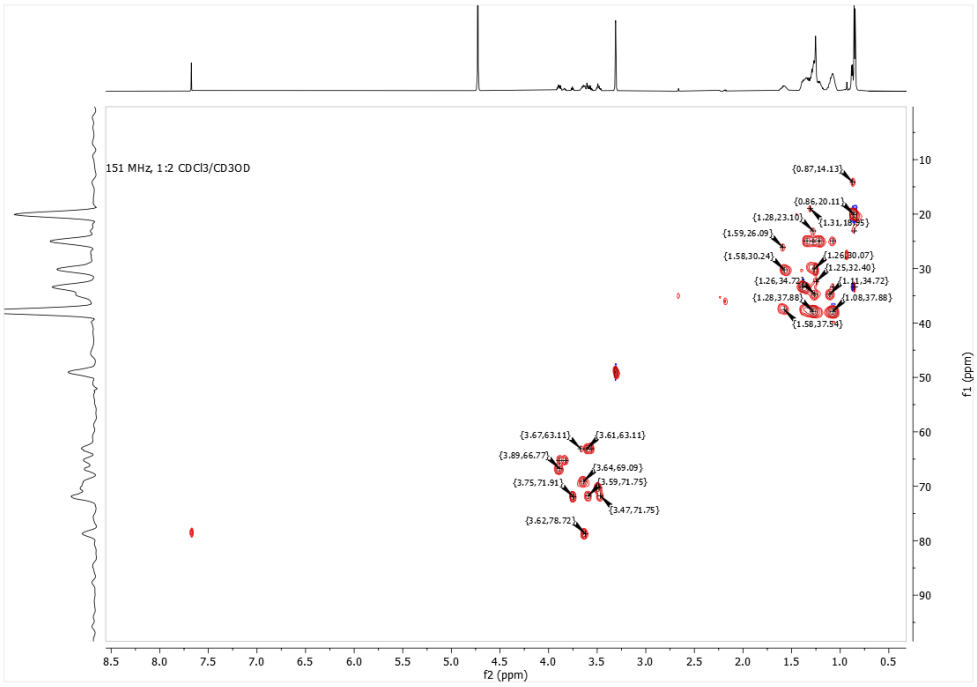

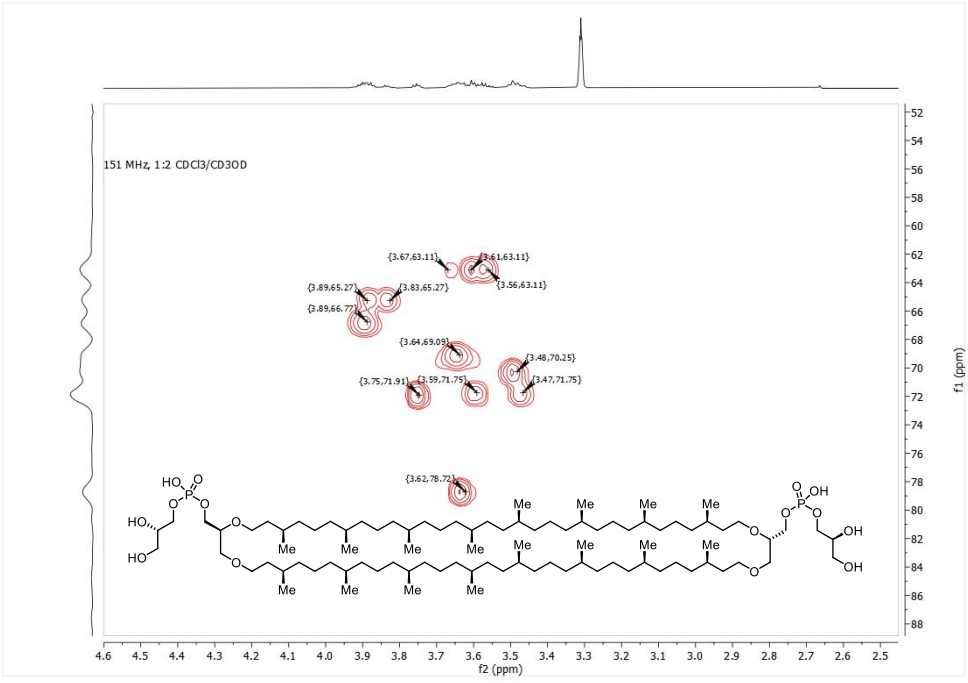

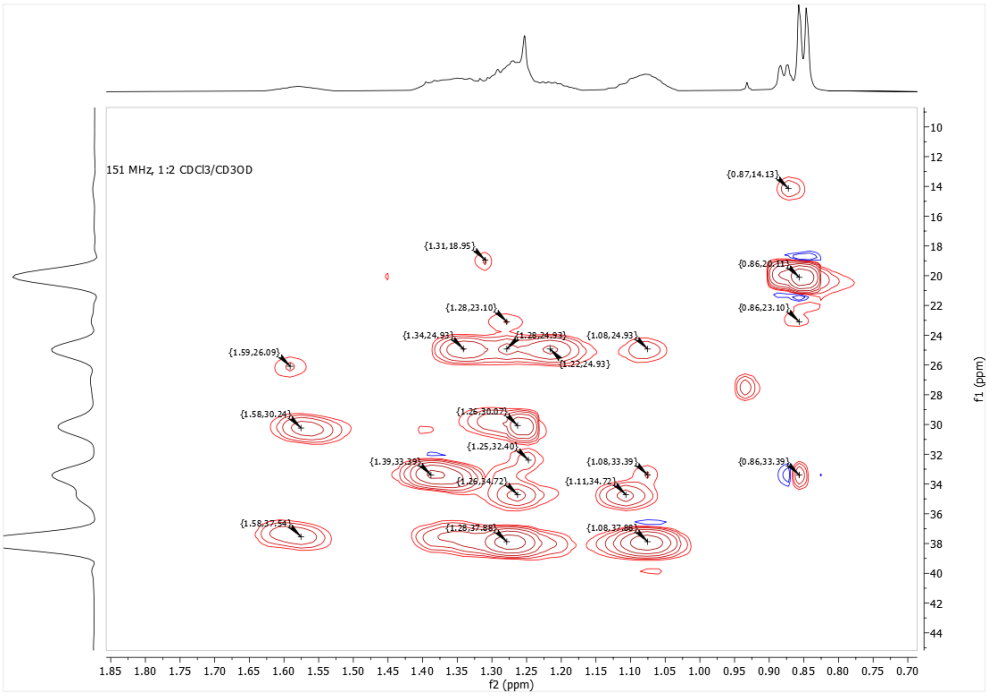

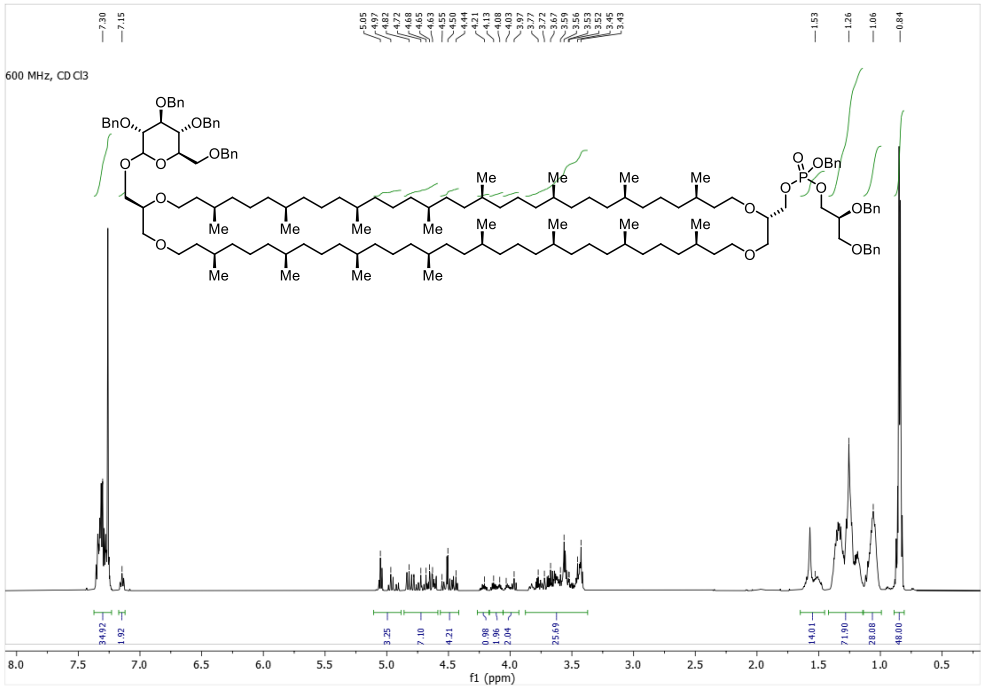

^{1}H NMR spectrum of compound **5**.

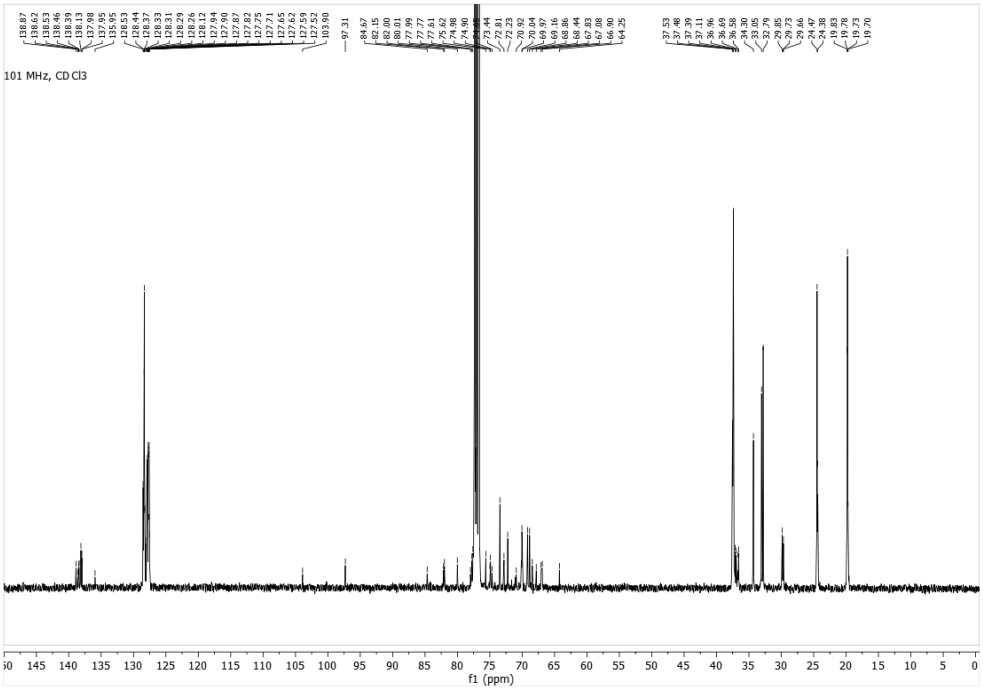

^{13}C NMR spectrum of compound **5.**

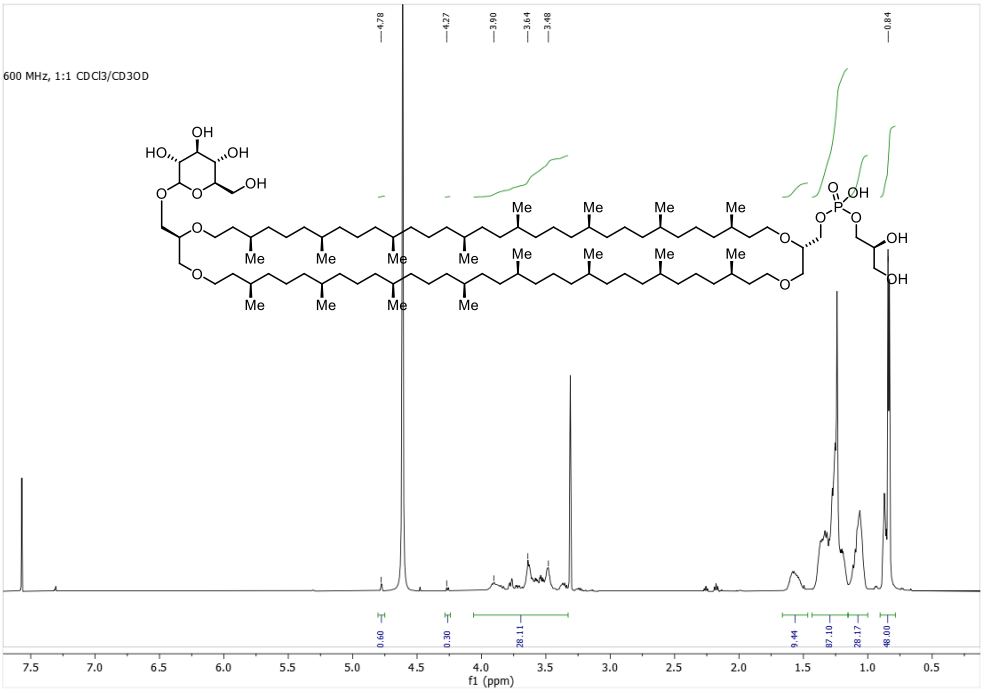

^{1}H NMR spectrum of compound **PG1Glc**.

HSQC Data for **PG1Glc**:

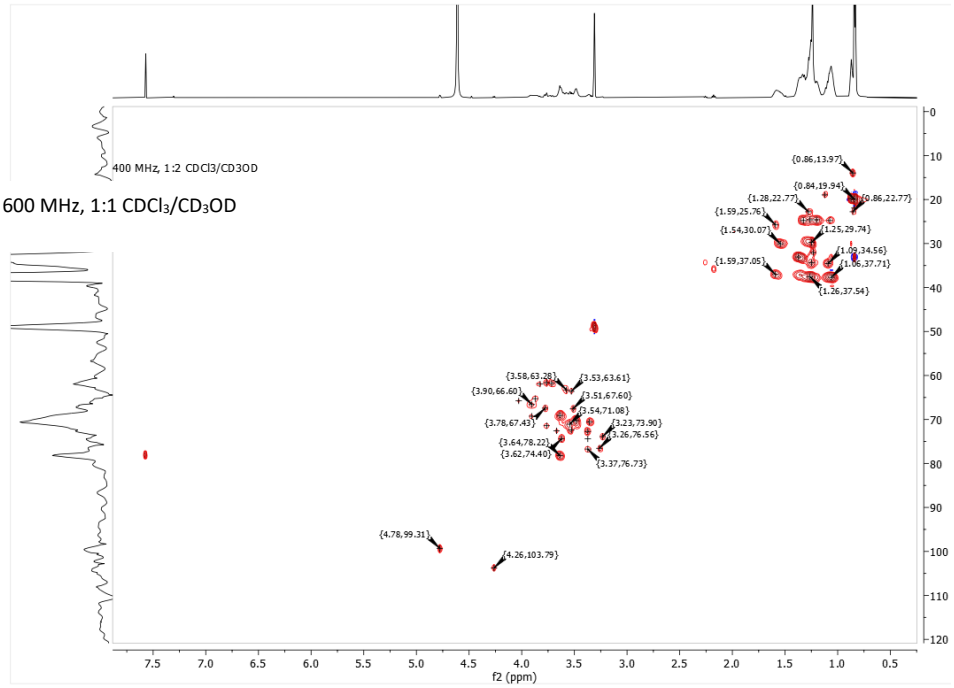

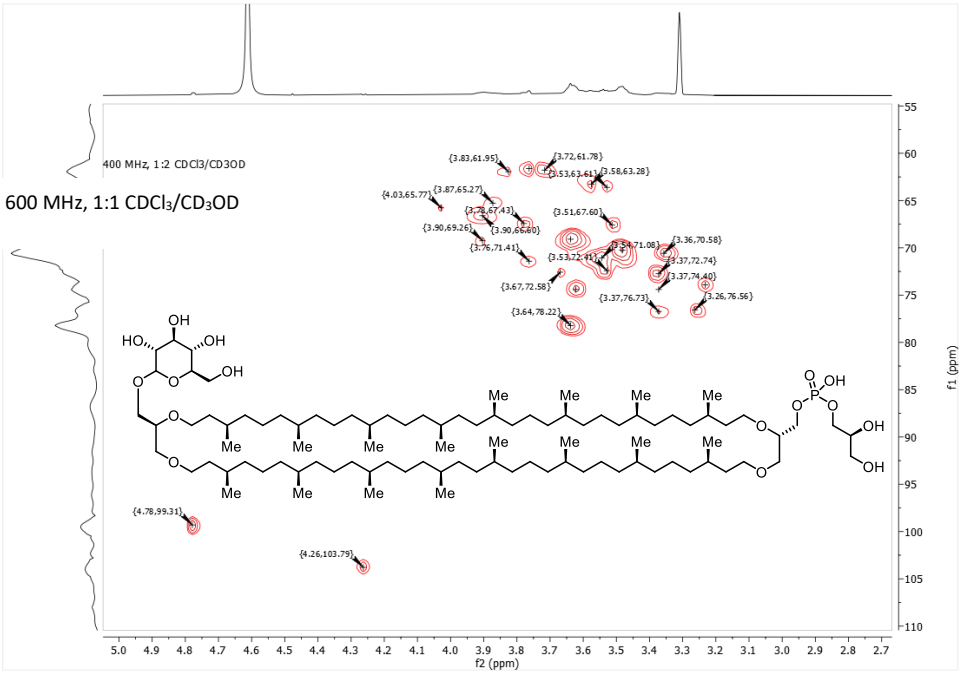

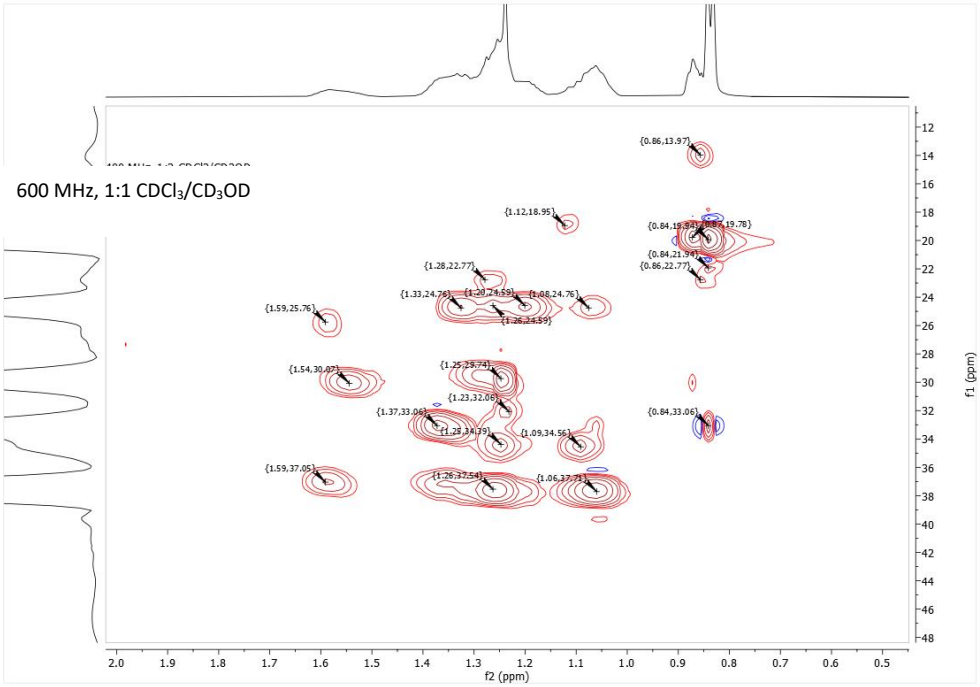

600 MHz, 1:1 $CDCl_3/CD_3OD$